BOX 1 | PREPARATION OF MEF FEEDERS

For maintenance of human ES cells, we use freeze-thawed MEF feeders. We treat MEFs with mitomycin C and prepare frozen stocks of the MEFs. One to two days before passage of human ES cells, frozen stocks of mitomycin C-treated MEF are thawed as feeders and should be used within 3 d.

Cyropresevation of mitomycin C-treated MEF feeders

1. Aspirate the media from a confluent 150-mm dish of MEFs. Add 25 ml of MEF media containing mitomycin C (final concentration: 10 μg ml^{-1}), and incubate the dish at 37 °C for 2 h.
2. Wash the dish with 15 ml of pre-warmed (37 °C) DMEM three times.
3. Add 25 ml of MEF media without mitomycin C, and incubate the dish overnight.
4. Aspirate the media, wash the dish with 20 ml of PBS add 5 ml of pre-warmed 0.25% (wt/vol) trypsin-EDTA and incubate the dish at 37 °C for 4 min.
5. Add 5 ml of MEF media into the dish, and dissociate the MEFs into single cells by pipetting. Transfer the cell suspension to a 50-ml conical tube.
6. To collect the remaining cells in the dish, add 10 ml of MEF media to the dish, and transfer the cell suspension into the 50-ml conical tube from Step 5.
7. Mix 50 μl of the cell suspension and 50 μl of 0.4% (wt/vol) Trypan blue, and calculate the total number of cells in the 50 ml tube
8. Centrifuge the 50 ml tube for 3 min at 180*g* at room temperature.
9. Aspirate the supernatant carefully and adjust the cell concentrations to 4.8×10^6 cells per ml with pre-cooled (4 °C) freezing solution.
10. Add 250 μl of the cell suspension to a cryovial.
11. Place the cryovials in a cell-freezing container and transfer the freezing container directly into −80 °C freezer.
12. The next day, transfer the cryovials into −150 °C freezer or liquid nitrogen.

Thawing of MEF feeders

13. 1–2 d before passage of human ES cells, thaw the cryovial in a 37 °C water bath with gentle agitation until most of the ice disappears.
14. Transfer the content of the cryovial to a 50-ml tube containing 20 ml of pre-warmed (37 °C) MEF media.
15. To collect the remaining cells in the cryovial, add 1 ml of MEF media to the cryovial with a P1000 micropipette, and transfer the cell suspension into the 50 ml conical tube from Step 14.
16. After gentle pipetting, centrifuge the 50 ml tube for 3 min at 180*g* at room temperature.
17. Aspirate the supernatant and suspend all the cells with 10 ml of pre-warmed MEF media.
18. Plate the cell suspension onto a gelatin-coated 100 mm dish.
19. Before passage of human ES cells, wash the MEF feeders twice with pre-warmed DMEF/F12 (at Step 2Bviii).

▲ **CRITICAL STEP** Freezing solutions contain DMSO. Higher concentrations of DMSO are toxic to cells. Freezing and thawing of cells should be as quickly as possible.

(vii) Adjust the concentration to 4.7×10^4 cells per ml with maintenance media containing LIF (final concentration: 2.0×10^3 unit ml^{-1}) and Blas (final concentration: 20 μg ml^{-1}).

(viii) Seed 9 ml of the cell suspension onto a gelatin-coated 100-mm dish (4.2×10^5 cells/100 ml dish), and incubate the dish at 37 °C in a humidified atmosphere of 5% CO_2.

(ix) After 2 d, the cells become confluent. Passage the cells using the same procedure described above in Steps A(i–viii).

(x) **Day 0: Start of ES cell differentiation.** Repeat Steps A(i–vi).

(xi) Adjust the cell concentration to 5.6×10^4 cells per ml with retinal progenitor differentiation media containing Dkk-1 (final concentration: 100 ng ml^{-1}) and Lefty-A (final concentration: 500 ng ml^{-1}), and seed 9 ml of the cell suspension onto a Petri dish (5.0×10^5 cells/100 mm dish).

(xii) Incubate the dish at 37 °C in a humidified atmosphere of 5% CO_2 for 72 h.

▲ **CRITICAL STEP** We recommend that the pH of the differentiation media be checked using the color of the phenol red. Old media turn pink or red because of the loss of CO_2, which causes low differentiation efficiency. We recommend using fresh media for differentiation.

? TROUBLESHOOTING

(xiii) **Day 3: Addition of factor and media change.** Observe the dish and confirm the formation of ES cell aggregates (**Fig. 4b**). Collect the media containing floating aggregates into a 15-ml tube.

(xiv) Leave the tube until the aggregates sink down to the bottom of the tube (~15 min).

(xv) Remove half of the media (4.5 ml), and add 4 ml of fresh differentiation media and 450 μl of FBS (final concentration: 5% (vol/vol)).

TABLE 1 | List of useful antibodies and reagents for staining.

Protein	Expression	Maker	No.	Host	Dilution
Oct3/4	Undifferentiated ES cells	BD	611202	Mouse	1:300
Nanog	Undifferentiated ES cells (mouse)	ReproCell	RCAB0001P	Rabbit	1:1,000
	Undifferentiated ES cells (human)	R&D	AF1997	Goat	1:20
TRA-1-60	Undifferentiated ES cells	Chemicon	MAB4360	Mouse (IgM)	1:300
TRA-1-81	Undifferentiated ES cells	Chemicon	MAB438	Mouse (IgM)	1:300
Nestin	Neural progenitors (mouse)	BD	556309	Mouse	1:1,000
	Neural progenitors (human)	Covance	PRB-570C	Rabbit	1:1,000
NCAM	Neurons	Chemicon	AB5032	Rabbit	1:200
βIII-Tubulin	Neurons	Sigma	T8660	Mouse	1:500
	Neurons	Covance	PRB-435P	Rabbit	1:600
Rx	Retinal progenitors	Gift	Dr. Sasai (RIKEN)	Rabbit	1:200
Mitf	Retinal progenitors	Abcam	ab2384	Mouse	1:30
Pax6	Retinal progenitors	DSHB		Mouse	1:200
	Retinal progenitors	Covance	PRB-278P	Rabbit	1:500
Chx10	Retinal progenitors	Exalpha	X1180P	Sheep	1:1,000
Crx	Photoreceptor precursors	Gift	Dr. Sasai (RIKEN)	Rat	1:200
Blue opsin	Cone photoreceptors	Chemicon	AB5407	Rabbit	1:500
Red/green opsin	Cone photoreceptors	Chemicon	AB5405	Rabbit	1:500
Rhodopsin	Rod photoreceptors	Sigma	04886	Mouse	1:2,000
Recoverin	Rod and cone photoreceptors	Chemicon	AB5585	Rabbit	1:2,000
ZO-1	Tight junctions	Zymed	61-7300	Rabbit	1:100
Phalloidin (Alexa488)	F-actin (polygonal morphology)	Invitrogen	A-12379		5 U ml^{-1}
Phalloidin (Alexa546)	F-actin (polygonal morphology)	Invitrogen	A-22283		5 U ml^{-1}

(xvi) Seed the cell suspension onto an MPC-treated dish and place in a 37 °C incubator with 5% CO_2. Culture the cells for 24 h.
▲ **CRITICAL STEP** After addition of FBS, cells become adherent. Therefore, MPC-treated dishes are recommended for floating culture.

(xvii) **Day 4: Addition of factor.** Add 18 μl of Activin-A (final concentration: 10 ng ml^{-1}) to the media and incubate at 37 °C in a humidified atmosphere of 5% CO_2. Culture the cells for 24 h.

(xviii) **Day 5: Media change.** Repeat Steps A(xiii) and (xiv).

(xix) Aspirate the media, and add 9 ml of fresh retinal progenitor differentiation media.

(xx) Plate the cell suspension onto a new MPC-treated dish and place in a 37 °C incubator with 5% CO_2. Culture the cells for 48 h.

(xxi) **Day 7: Media change.** Repeat Steps A(xviii) to (xx) (**Fig. 4c**).

(xxii) **Day 9: FACS analysis.** Repeat Steps A(xiii) and (xiv).

(xxiii) Aspirate the media, add 1 ml of 0.25% (vol/vol) trypsin-EDTA, collect the cells and centrifuge for 3 min at 180*g* at room temperature.

(xxiv) Aspirate the supernatant, add 1 ml of 0.25% (vol/vol) trypsin-EDTA, place the tube at 37 °C for 5 min. Mix the contents gently every 2 min.
▲ **CRITICAL STEP** KSR in the culture media prevent trypsin reaction. Before reaction with 0.25% (vol/vol) trypsin-EDTA, the cells are washed with 0.25% (vol/vol) trypsin-EDTA once to remove KSR.

(xxv) Pipette gently ~20 times to dissociate aggregates into single cells.

(xxvi) Transfer the cell suspension to a 1.5-ml tube, and add 500 μl of DMEM containing 10% (vol/vol) FBS and 6 μl of DNase I (10 μg ml^{-1}). Pipette gently ~10 times.

(xxvii) Centrifuge at for 3 min at 200*g* at 4 °C.

(xxviii) Aspirate the supernatant and add 800 μl of 0.5 μg ml^{-1} PI-containing buffer (9 ml PBS, 1 ml of 1% (wt/vol) BSA–PBS and 5 μl of PI solution).

(xxix) Pass the cell suspension through a cell strainer (35-μm nylon mesh) to remove cell aggregates and DNA debris. Place the tube on ice until FACS analysis.

(xxx) Collect GFP+ cells using a FACSAria (**Fig. 4d**). Count Rx-GFP+ cells with GFP fluorescence and sort using a 530-nm band pass filter (FITC). Exclude cell aggregates and PI-positive cells by adjusting gating parameters for forward scatter and side scatter and using a 695-nm band pass filter (PerCP-Cy5.5). Analyze data using FACSDiva software.

(xxxi) Transfer 2–3 × 10^4 sorted cells to a 1.5-ml tube and centrifuge at for 3 min at 200*g* at 4 °C.
▲ **CRITICAL STEP** The number of reaggregated pellets obtained depends on the differentiation efficiency. Higher efficiency requires preparation of more 1.5-ml tubes of cells.
? TROUBLESHOOTING

(xxxii) Aspirate the supernatant and resuspend the cells in 100 µl of retinal cell differentiation media containing 10% (vol/vol) FBS, and centrifuge for 10 min at 800*g* at room temperature to produce a reaggregation pellet.

(xxxiii) Let the tube sit at 37 °C in a humidified atmosphere of 5% CO_2 for 1 h.
▲ **CRITICAL STEP** Treat the tube gently to avoid the collapse of reaggregation pellets. Do not shake the tube.

(xxxiv) Plate 3–5 reaggregated pellets into one well of an eight-well chamber slide coated with poly-D-lysine, laminin and fibronectin using a wide-tip pipette. Incubate the pellets in retinal cell differentiation media containing 10% (vol/vol) FBS.
▲ **CRITICAL STEP** Use wide-tip pipettes, as narrow-tip pipettes collapse the reaggregation pellets. Survival of single cells is low.

(xxxv) Incubate the slide at 37 °C in a humidified atmosphere of 5% CO_2. Culture for 24 h.

(xxxvi) **Days 10, 12 and 14: Media change.** Aspirate the media gently and add 500 µl of retinal cell differentiation media containing DAPT (10 µM) but not FBS.

(xxxvii) Incubate the slide at 37 °C in a humidified atmosphere of 5% CO_2. Culture for 48 h.

(xxxviii) Repeat Steps A(xxxvi) and (xxxvii).

(xxxix) Repeat Steps A(xxxvi) and (xxxvii).

(xl) **Days 16, 18, 20 and 22: Media change.** Aspirate the media gently and add 500 µl of retinal cell differentiation media containing DAPT (10 µM), aFGF (50 ng ml^{-1}), bFGF (10 ng ml^{-1}), Shh (3 nM), RA (500 nM) and taurine (100 µM).

(xli) Incubate the slide at 37 °C in a humidified atmosphere of 5% CO_2. Culture for 48 h.

(xlii) **Days 24, 26 and 28: Media change.** Aspirate the media gently and add retinal cell differentiation media containing DAPT (10 µM), Shh (3 nM), RA (500 nM) and taurine (100 µM).

(xliii) Incubate the slide at 37 °C in a humidified atmosphere of 5% CO_2. Culture for 48 h.

(xliv) Repeat Steps A(xlii) and (xliii) three times to change the media every other day (**Fig. 5**). Culture for a total of 28 d (**Fig. 6**).
? TROUBLESHOOTING

(B) Retinal differentiation of human ES cells (day 0: maintenance and passaging of cells ● TIMING 1.5 h)

(i) Prepare mitomycin C-treated MEFs as feeder layers for the culture of human ES cells (**Box 1**).

(ii) Aspirate the media from a 100-mm dish of human ES cells and wash with 9 ml of pre-warmed PBS (37 °C). Aspirate the PBS, and add 2 ml of pre-warmed human ES cell dissociation solution.

(iii) Incubate at 37 °C for 5–7 min and tap the dish every 2 min.

(iv) Examine the cells by inverted microscopy to confirm that most ES cell colonies have partially detached from the substratum (**Fig. 7**). Add 2 ml of human ES cell maintenance media to detach ES colonies with gentle pipetting, and transfer the ES cell suspension into a 15-ml tube.

(v) Add 2 ml of human ES cell maintenance media to the dish, detach remaining ES colonies with gentle pipetting and transfer the ES cell suspension into the same 15-ml tube.

(vi) Dissociate the ES colonies into clusters of ~50 cells with gentle pipetting.

(vii) Centrifuge for 5 min at 180*g* at room temperature.

(viii) Meanwhile, prepare three new dishes of MEF feeders for a 1:3 split. Wash the feeders twice with DMEM/F12, add 8 ml of maintenance media and apply 10 µl of bFGF solution (final concentration 5 ng ml^{-1}) to each dish.

(ix) Aspirate the supernatant of the tube of cells from Step B(vii), and add 6 ml of maintenance media to resuspend the ES cells for the 1:3 split.

(x) Dispense 2 ml of the cell suspension into each of the three maintenance media-containing feeder dishes prepared in Step B(viii) (total volume of media in the dish is 10 ml).

(xi) Incubate the dish at 37 °C in a humidified atmosphere of 2% CO_2 and 98% air.

(xii) Change the media daily. Human ES cells should be passaged every 3–4 d.

(xiii) **Day 0: Start of ES cell differentiation.** To a confluent dish of ES cells, apply 10 µl of Y-27632 (final concentration: 10 µM), and incubate the dish at 37 °C for 1 h in a humidified atmosphere of 2% CO_2.

(xiv) Aspirate the media from the dish and add 9 ml of pre-warmed PBS. Aspirate the PBS and add 2 ml of pre-warmed human ES cell dissociation solution. Incubate the dish at 37 °C for 5–7 min.

(xv) Examine the cells by inverted microscopy, and confirm that most ES cell colonies have partially detached from the substratum. Add 2 ml of maintenance media and detach the ES colonies with gentle pipetting. Transfer the ES cell suspension into a 15-ml tube.

(xvi) Dissociate the ES colonies into clusters of ~30–40 cells with gentle pipetting.

(xvii) Add 2 ml of maintenance media to detach the remaining ES colonies, and collect the ES colonies in the same 15-ml tube.

(xviii) Centrifuge for 5 min at 180*g* at room temperature.

(xix) Aspirate the supernatant and resuspend with 9 ml of human ES cell maintenance media containing Y-27632 (10 μM).

(xx) Dissociate the colonies into 3–10 cells by gentle pipetting.

▲ **CRITICAL STEP** Dissociation of human ES cells to single cells markedly decreases cell viability, although Y-27632 protects from dissociation-induced cell death. Pipette gently, as excessive, forceful and repetitive pipetting or formation of air bubbles during pipetting decreases cell viability.

(xxi) Plate the cell suspension onto gelatin-coated dishes to remove the MEFs, and incubate the dish at 37 °C for 1 h.

▲ **CRITICAL STEP** MEFs adhere more quickly to the dish than do human ES cells, so incubating the dish at 37 °C for 1 h will allow the MEFs to settle, while ES cells remain floating.

(xxii) Collect the supernatant with the floating ES cells into a 50-ml tube, and centrifuge for 3 min at 180*g* at room temperature.

(xxiii) Aspirate the supernatant and add 2 ml of maintenance media.

(xxiv) Seed the 50 μl of the cell suspension onto the dish, and count the total number of clumps in 50 μl of the cell suspension without Trypan blue staining.

(xxv) Seed the cells onto MPC-treated non-adhesive dishes at a density of 6,000 cells in 9 ml of media containing Y-27632 (10 μM), Dkk-1 (100 ng ml^{-1}) and Lefty-A (500 ng ml^{-1}). Incubate the dish at 37 °C in a humidified atmosphere of 5% CO_2.

▲ **CRITICAL STEP** We recommend that the pH of the differentiation media be checked on the basis of the color of the phenol red. Old media turn pink or red because of the loss of CO_2, which causes low differentiation efficiency. We recommend using fresh media for differentiation.

? TROUBLESHOOTING

(xxvi) **Day 3: Media change with 20% (vol/vol) KSR differentiation media.** Collect the supernatant in a 50-ml tube and centrifuge for 3 min at 180*g* at room temperature.

(xxvii) Discard the upper half of the media and add 4.5 ml of 20% (vol/vol) KSR differentiation media containing Y-27632 (10 μM), Dkk-1 (100 ng ml^{-1}) and Lefty-A (500 ng ml^{-1}).

(xxviii) Plate the cell suspension onto a new MPC-treated dish and incubate the dish at 37 °C in a humidified atmosphere of 5% CO_2. Culture the cells for 72 h (**Fig. 8a**).

▲ **CRITICAL STEP** We recommend that the pH of the differentiation media be checked on the basis of the color of the phenol red. Old media turn pink or red because of the loss of CO_2, which causes low differentiation efficiency. We recommend using fresh media for differentiation.

? TROUBLESHOOTING

(xxix) **Days 6, 9 and 12: Media change with 15% KSR differentiation media.** Collect the supernatant in a 15-ml tube and centrifuge for 3 min at 180*g* at room temperature.

(xxx) Discard the upper half of the media and add 4.5 ml of 15% (vol/vol) KSR differentiation media containing Y-27632 (10 μM), Dkk-1 (100 ng ml^{-1}) and Lefty-A (500 ng ml^{-1}).

(xxxi) Plate the cell suspension in a new MPC-treated dish and incubate the dish at 37 °C in a humidified atmosphere of 5% CO_2. Culture the cells for 72 h.

(xxxii) Repeat Steps B(xxix–xxxi) twice.

? TROUBLESHOOTING

(xxxiii) **Days 15 and 18: Media change with 10% KSR differentiation media.** Collect the supernatant in a 50-ml tube and let the tube stand for 20 min.

▲ **CRITICAL STEP** Confirm that the aggregates sink down to the bottom of the tube.

(xxxiv) Discard the upper half of the media and add 4.5 ml of 10% (vol/vol) KSR differentiation media containing Dkk-1 (100 ng ml^{-1}) and Lefty-A (500 ng ml^{-1}).

(xxxv) Plate the cell suspension onto a new MPC-treated dish and incubate the dish at 37 °C in a humidified atmosphere of 5% CO_2. Culture the cells for 72 h (**Fig. 8b**).

(xxxvi) Repeat Steps B(xxxiii–xxxv).

? TROUBLESHOOTING

(xxxvii) **Day 21: Seed the aggregates onto poly-D-lysine/laminin/fibronectin-coated dishes.** Repeat Steps B(xxxiii) and (xxxiv).

(xxxviii) Transfer the aggregates to poly-D-lysine/laminin/fibronectin-coated chamber slides at 10–20 aggregates per well.

(xxxix) Incubate the slides at 37 °C in a humidified atmosphere of 5% CO_2. Culture the cells for 72 h.

(xl) **Days 24–40: Media change every other day.** Remove the media gently.
(xli) Gently add 500 µl of fresh 10% (vol/vol) KSR differentiation media to each well.
(xlii) Incubate the dish at 37 °C in a humidified atmosphere of 5% CO_2 for 48 h (**Fig. 9**).
(xliii) Repeat Steps B(xl–xlii) nine times so that the cells are cultured for a total of 40 d.
? TROUBLESHOOTING
(xliv) **Days 41–90: Media change every day.** Gently remove the media from the 40 d ES cells, and add 500 µl of fresh 10% KSR differentiation media to each well.
(xlv) Incubate the dish at 37 °C in a humidified atmosphere of 5% CO_2.
(xlvi) Repeat Steps B(xliv) and (xlv) every 24 h so that the cells have been cultured for another 50 d (total 90 d of culture).
? TROUBLESHOOTING

3| Human ES Cells can be differentiated into RPE cells using option A or into photoreceptor cells using option B.

(A) Differentiation into RPE cells (days 91–120: media change every day ● TIMING 1 h plus 30 d of culture)
(i) Gently remove the media from the 91 d ES cells and add 500 µl of fresh 10% KSR differentiation media to each well.
(ii) Incubate the dish at 37 °C in a humidified atmosphere of 5% CO_2.
(iii) In order to obtain mature RPE cells, repeat Steps 3A(i) and (ii) every 24 h so that the cells have been cultured for another 30 d (total 120 d of culture) (**Figs. 10** and **11**).
? TROUBLESHOOTING

(B) Differentiation into photoreceptor cells (days 91–150: Media change every day ● TIMING 1 h plus 60 d of culture)
(i) Gently remove the media from the 91 d ES cells and add 500 µl of photoreceptor differentiation media containing retinoic acid (100 nM) and taurine (100 M).
(ii) Incubate the dish at 37 °C in a humidified atmosphere of 5% CO_2.
(iii) Repeat Steps 3B(i) and (ii) every day for another 60 d (total 150 d of culture) (**Figs. 12** and **13**).
? TROUBLESHOOTING

● TIMING
Step 2(A) Differentiation of mouse ES cells: 28 d
Step 2(B) Differentiation of human ES cells: 90 d
Step 3(A) Differentiation of human ES cells into RPE cells: 30 d (total 120 d)
Step 3(B) Differentiation of human ES cells into photoreceptor cells: 60 d (total 150 d)

? TROUBLESHOOTING
Troubleshooting advice can be found in **Table 2**.

TABLE 2 | Troubleshooting table.

Step	Problem	Possible reason	Possible solution
2A(xii)	Mouse ES cells do not form aggregates	Use of wrong media and reagents. Initially, ES cells were not normal and did not retain pluripotency	Ensure proper preparation of media and reagents. Media, KSR and supplements must be fresh. Check the pluripotency by RT-PCR for pluripotency factors or by immunostaining for Oct3/4 and Nanog. Use a new frozen stock of ES cells at an early passage number
2A(xxxi)	The number of the FACS-sorted cells is low	Differentiation efficiency is low	Ensure the media and reagents. Media, KSR and supplements must be fresh. Check the pluripotency by RT-PCR for pluripotency factors or by immunostaining for Oct3/4 and Nanog. Use a new frozen stock of ES cells at early passage number. Try a different ES cell line
		Cell viability is low. Repetitive pipetting force is too high during dissociation. Formation of air bubbles during repetitive pipetting. Cell viability gradually decreases with increased sorting time	Pipetting should be gentle. Sorting duration should be <4 h

(continued)

TABLE 2 | Troubleshooting table (continued).

Step	Problem	Possible reason	Possible solution
2B(xxv), (xxviii), (xxxii) and (xxxvi)	Human ES cells do not form aggregates Low survival in floating cultures	Repetitive pipetting force is too high during dissociation. Formation of air bubbles during repetitive pipetting. Too many cells or too many colonies plated	Ensure the preparation of media and reagents. Pipetting should be gentle. Add Y-27632 at a higher concentration and/or for a longer period of time. Optimize the density by serial dilution of cells or colonies
2B(xliii), (xlvi), 3A(iii) and 3B(iii)	Low survival in cell cultures after replating	Culture surface is not adequate. Too many colonies plated	Use cell culture grade glass slides and coat them with poly-D-lysine, laminin and fibronectin. Ensure preparation of media and regents. Optimize the density by serial dilution of colonies
2A(xliv), 3A(iii) and 3B(iii)	ES cells do not differentiate into retinal cells	Initially, ES cells were not normal and did not retain pluripotency. Use of old media and reagents	Check for the generation of retinal progenitors. Expression of retinal progenitor markers should be examined on days 8–10 and days 30–40 in mouse and human ES cells, respectively Ensure that the media and reagents support self-renewal. Media, KSR and supplements must be fresh. Check the pluripotency by immunostaining for Oct3/4, Nanog, TRA-1-60 and TRA-1-81, or by RT-PCR for pluripotency factors Use a new frozen stock of ES cells at early passage number. Try a different ES cell line

ANTICIPATED RESULTS

When differentiating mouse ES cells (**Fig. 3a**), under optimal conditions, 10–20% of cells become Rx-GFP+, as evaluated by FACS (**Fig. 4**). Expression of the retinal progenitor markers Rx, Mitf and Pax6 are detected between days 8 and 12, with 20–30% of colonies positive for Rx/Pax6 (neural retina progenitors) or Mitf/Pax6 (RPE progenitors) (**Fig. 2**). For mature phenotypes, 25–35% of sorted cells are positive for rhodopsin, red/green opsin or blue opsin in mouse ES cell cultures between days 28 and 40 (**Figs. 2** and **6**). Under the same conditions, Mitf+ RPE cells are observed in 20–30% of sorted cells.

For human ES cells (**Fig. 3b**), expression of Rx, Mitf and Pax6 is detected between days 30 and 45, with 20–30% of colonies positive for Rx/Pax6 or Mitf/Pax6 (**Figs. 2, 8** and **9**). Prolonged culture generates mature RPE cells at 25–35% of total colonies between days 50 and 120, as determined by staining for Mitf, ZO-1 and F-actin. Pigmentation is observed starting at ~40 d. More mature RPE cells with a polygonal shape require longer culture (more than 90 d) (**Figs. 2, 10** and **11**). For photoreceptor differentiation, addition of RA and taurine induces 10–20% of cells to become positive for rhodopsin, red/green opsin or blue opsin between days 120 and 200 (**Figs. 2, 12** and **13**). These cells express genes responsible for phototransduction in rods and/or cones.

ACKNOWLEDGMENTS We thank H. Suemori and N. Nakatsuji (Kyoto University) for providing the human ES cell line; K. Watanabe, M. Ueno and N. Osakada for valuable comments; and members of the Takahashi laboratory, the Sasai laboratory and the Akaike laboratory for helpful discussions and technical assistance. This work was supported by Grants-in-Aid from the Ministry of Education, Culture, Sports, Science and Technology, and the Leading Project (M.T. and Y.S.). This study was also supported by Grants-in-Aid for Scientific Research from the Japan Society for the Promotion of Science and the Mochida Memorial Foundation for Medical and Pharmaceutical Research (F.O.).

Published online at http://www.natureprotocols.com/
Reprints and permissions information is available online at http://npg.nature.com/reprintsandpermissions/

1. Evans, M.J. & Kaufman, M.H. Establishment in culture of pluripotential cells from mouse embryos. *Nature* **292**, 154–156 (1981).
2. Zhao, C., Deng, W. & Gage, F.H. Mechanisms and functional implications of adult neurogenesis. *Cell* **132**, 645–660 (2008).
3. Ooto, S. *et al.* Potential for neural regeneration after neurotoxic injury in the adult mammalian retina. *Proc. Natl Acad. Sci. USA* **101**, 13654–13659 (2004).
4. Osakada, F. *et al.* Wnt signaling promotes regeneration in the retina of adult mammals. *J. Neurosci.* **27**, 4210–4219 (2007).
5. Lindvall, O. & Kokaia, Z. Stem cells for the treatment of neurological disorders. *Nature* **441**, 1094–1096 (2006).
6. Hartong, D.T., Berson, E.L. & Dryja, T.P. Retinitis pigmentosa. *Lancet* **368**, 1795–1809 (2006).

7. Rattner, A. & Nathans, J. Macular degeneration: recent advances and therapeutic opportunities. *Nat. Rev. Neurosci.* **7**, 860–872 (2006).
8. Haruta, M. *et al.* *In vitro* and *in vivo* characterization of pigment epithelial cells differentiated from primate embryonic stem cells. *Invest. Ophthalmol. Vis. Sci.* **45**, 1020–1025 (2004).
9. Lund, R.D. *et al.* Human embryonic stem cell-derived cells rescue visual function in dystrophic RCS rats. *Cloning Stem Cells* **8**, 189–199 (2006).
10. MacLaren, R.E. *et al.* Retinal repair by transplantation of photoreceptor precursors. *Nature* **444**, 203–207 (2006).
11. Tropepe, V. *et al.* Retinal stem cells in the adult mammalian eye. *Science* **287**, 2032–2036 (2000).
12. Haruta, M. *et al.* Induction of photoreceptor-specific phenotypes in adult mammalian iris tissue. *Nat. Neurosci.* **4**, 1163–1164 (2001).
13. Takahashi, K. & Yamanaka, S. Induction of pluripotent stem cells from mouse embryonic and adult fibroblast cultures by defined factors. *Cell* **126**, 663–676 (2006).
14. Takahashi, K. *et al.* Induction of pluripotent stem cells from adult human fibroblasts by defined factors. *Cell* **131**, 861–872 (2007).
15. Yu, J. *et al.* Induced pluripotent stem cell lines derived from human somatic cells. *Science* **318**, 1917–1920 (2007).
16. Lamba, D., Karl, M. & Reh, T. Neural regeneration and cell replacement: a view from the eye. *Cell Stem Cell* **2**, 538–549 (2008).
17. Lamba, D.A., Gust, J. & Reh, T.A. Transplantation of human embryonic stem cell-derived photoreceptors restores some visual function in crx-deficient mice. *Cell Stem Cell* **4**, 73–79 (2009).
18. Osakada, F. & Takahashi, M. Drug development targeting the glycogen synthase kinase-3beta (GSK-3beta)-mediated signal transduction pathway: targeting the Wnt Pathway and transplantation therapy as strategies for retinal repair. *J. Pharmacol. Sci.* **109**, 168–173 (2009).
19. Wichterle, H., Lieberam, I., Porter, J.A. & Jessell, T.M. Directed differentiation of embryonic stem cells into motor neurons. *Cell* **110**, 385–397 (2002).
20. Mizuseki, K. *et al.* Generation of neural crest-derived peripheral neurons and floor plate cells from mouse and primate embryonic stem cells. *Proc. Natl Acad. Sci. USA* **100**, 5828–5833 (2003).
21. Watanabe, K. *et al.* Directed differentiation of telencephalic precursors from embryonic stem cells. *Nat. Neurosci.* **8**, 288–296 (2005).
22. Adler, R. & Canto-Soler, M.V. Molecular mechanisms of optic vesicle development: complexities, ambiguities and controversies. *Dev. Biol.* **305**, 1–13 (2007).
23. Osakada, F. & Takahashi, M. Retinal regeneration by somatic stem cells. *Exp. Med.* **24**, 256–262 (2006).
24. Marquardt, T. & Gruss, P. Generating neuronal diversity in the retina: one for nearly all. *Trends Neurosci.* **25**, 32–38 (2002).
25. Ikeda, H. *et al.* Generation of Rx+/Pax6+ neural retinal precursors from embryonic stem cells. *Proc. Natl Acad. Sci. USA* **102**, 11331–11336 (2005).
26. Osakada, F. *et al.* Toward the generation of rod and cone photoreceptors from mouse, monkey and human embryonic stem cells. *Nat. Biotechnol.* **26**, 215–224 (2008).
27. Thomson, J.A. *et al.* Embryonic stem cell lines derived from human blastocysts. *Science* **282**, 1145–1147 (1998).
28. Bain, G., Kitchens, D., Yao, M., Huettner, J.E. & Gottlieb, D.I. Embryonic stem cells express neuronal properties *in vitro*. *Dev. Biol.* **168**, 342–357 (1995).
29. Kawasaki, H. *et al.* Induction of midbrain dopaminergic neurons from ES cells by stromal cell-derived inducing activity. *Neuron* **28**, 31–40 (2000).
30. Lee, S.H., Lumelsky, N., Studer, L., Auerbach, J.M. & McKay, R.D. Efficient generation of midbrain and hindbrain neurons from mouse embryonic stem cells. *Nat. Biotechnol.* **18**, 675–679 (2000).
31. Ying, Q.L., Stavridis, M., Griffiths, D., Li, M. & Smith, A. Conversion of embryonic stem cells into neuroectodermal precursors in adherent monoculture. *Nat. Biotechnol.* **21**, 183–186 (2003).
32. Barberi, T. *et al.* Neural subtype specification of fertilization and nuclear transfer embryonic stem cells and application in parkinsonian mice. *Nat. Biotechnol.* **21**, 1200–1207 (2003).
33. Ueno, M. *et al.* Neural conversion of ES cells by an inductive activity on human amniotic membrane matrix. *Proc. Natl Acad. Sci. USA* **103**, 9554–9559 (2006).
34. Kawasaki, H. *et al.* Generation of dopaminergic neurons and pigmented epithelia from primate ES cells by stromal cell-derived inducing activity. *Proc. Natl Acad. Sci. USA* **99**, 1580–1585 (2002).
35. Klimanskaya, I. *et al.* Derivation and comparative assessment of retinal pigment epithelium from human embryonic stem cells using transcriptomics. *Cloning Stem Cells* **6**, 217–245 (2004).
36. Zhao, X., Liu, J. & Ahmad, I. Differentiation of embryonic stem cells into retinal neurons. *Biochem. Biophys. Res. Commun.* **297**, 177–184 (2002).
37. Hirano, M. *et al.* Generation of structures formed by lens and retinal cells differentiating from embryonic stem cells. *Dev. Dyn.* **228**, 664–671 (2003).
38. Lamba, D.A., Karl, M.O., Ware, C.B. & Reh, T.A. Efficient generation of retinal progenitor cells from human embryonic stem cells. *Proc. Natl Acad. Sci. USA* **103**, 12769–12774 (2006).
39. Pouton, C.W. & Haynes, J.M. Embryonic stem cells as a source of models for drug discovery. *Nat. Rev. Drug Discov.* **8**, 605–616 (2007).
40. Nishikawa, S., Goldstein, R.A. & Nierras, C.R. The promise of human induced pluripotent stem cells for research and therapy. *Nat. Rev. Mol. Cell Biol.* **9**, 725–729 (2008).
41. Park, I.H. *et al.* Disease-specific induced pluripotent stem cells. *Cell* **134**, 877–886 (2008).
42. Ebert, A.D. *et al.* Induced pluripotent stem cells from a spinal muscular atrophy patient. *Nature* (2008).
43. Watanabe, T. & Raff, M.C. Rod photoreceptor development *in vitro*: intrinsic properties of proliferating neuroepithelial cells change as development proceeds in the rat retina. *Neuron* **4**, 461–467 (1990).
44. Levine, E.M., Fuhrmann, S. & Reh, T.A. Soluble factors and the development of rod photoreceptors. *Cell. Mol. Life Sci.* **57**, 224–234 (2000).
45. Suemori, H. *et al.* Efficient establishment of human embryonic stem cell lines and long-term maintenance with stable karyotype by enzymatic bulk passage. *Biochem. Biophys. Res. Commun.* **345**, 926–932 (2006).
46. Watanabe, K. *et al.* A ROCK inhibitor permits survival of dissociated human embryonic stem cells. *Nat. Biotechnol.* **25**, 681–686 (2007).
47. Wataya, T. *et al.* Minimization of exogenous signals in ES cell culture induces rostral hypothalamic differentiation. *Proc. Natl. Acad. Sci. USA* **105**, 11796–11801 (2008).
48. Fukuda, H. *et al.* Fluorescence-activated cell sorting-based purification of embryonic stem cell-derived neural precursors averts tumor formation after transplantation. *Stem Cells* **24**, 763–771 (2006).

Neuroscience Letters 458 (2009) 126–131

Contents lists available at ScienceDirect

Neuroscience Letters

journal homepage: www.elsevier.com/locate/neulet

Generation of retinal cells from mouse and human induced pluripotent stem cells

Yasuhiko Hirami[a,b], Fumitaka Osakada[a], Kazutoshi Takahashi[c,d], Keisuke Okita[c,d], Shinya Yamanaka[c,d], Hanako Ikeda[b], Nagahisa Yoshimura[b], Masayo Takahashi[a,*]

[a] Laboratory for Retinal Regeneration, RIKEN Center for Developmental Biology, 2-2-3 Minatojima-minamimachi, Chuo-ku, Kobe 650-0047, Japan
[b] Department of Ophthalmology, Kyoto University Graduate School of Medicine, Japan
[c] Department of Stem Cell Biology, Institute for Frontier Medical Sciences, Kyoto University, Japan
[d] Center for iPS Cell Research and Application (CiRA), Institute for Integrated Cell-Material Sciences, Kyoto University, Japan

ARTICLE INFO

Article history:
Received 9 January 2009
Received in revised form 15 April 2009
Accepted 15 April 2009

Keywords:
Differentiation
Induced pluripotent stem cell
Photoreceptor
Retinal pigment epithelium

ABSTRACT

We previously reported a technique for generating retinal pigment epithelia (RPE) and putative photoreceptors from embryonic stem (ES) cells. Here we tested whether our procedure can promote retinal differentiation of mouse and human induced pluripotent stem cells (iPSCs). Treating iPSCs with Wnt and Nodal antagonists in suspension culture induced expression of markers of retinal progenitor cells and generated RPE cells. Subsequently, treatment with retinoic acid and taurine generated cells positive for photoreceptor markers in all but one human cell lines. We propose that iPSCs can be induced to differentiate into retinal cells which have a possibility to be used as patient-specific donor cells for transplantation therapies.

Retinal degenerative diseases cause photoreceptor cell death and severely impair vision. Transplantation of retinal photoreceptors or RPE cells is a potential treatment to restore visual function. Although embryonic stem (ES) cells are potential donor cells for cell transplantation, clinical applications for these cells have drawbacks such as immune rejection. Induced pluripotent stem cells (iPSCs) are an alternative source of the donor cells. These ES-like cells are generated by reprogramming somatic cells through the retroviral activation of ES cell specific factors such as the four factors Oct3/4, Sox2, Klf4, and c-Myc and raise the possibility of treating patients with their own iPS cell-derived retinal cells which may resolve the problem of immune rejection [12,15,16].

Previously, we generated putative photoreceptors and RPE cells from rodent and primate ES cells using step-wise induction with defined factors [6,13]. During development of the vertebrate eye, the transcription factor gene Rx is expressed in progenitors of the neural retina [4,9], whereas the basic-helix-loop-helix-zipper transcription factor gene Mitf is expressed in the presumptive RPE [11]. At a later stage of differentiation in the neural retina, photoreceptor precursors express the homeobox gene Crx [2,5]. Finally, mature photoreceptors express recoverin and rhodopsin. ES cells differentiating into retinal cells *in vitro* also express this progression of retinal markers [6,13]. Here we tested whether iPSCs can be differentiated into retinal progenitors, RPE and photoreceptors with the same procedure used for ES cell differentiation.

All experiments in this study were conducted using mouse Nanog-iPS cell line iPS-MEF-Ng-20D-17 which were induced from mouse embryonic fibroblasts by retroviral transfection of Oct3/4, Sox2, Klf4, and c-Myc [12], human iPS cell lines 201B6 and 201B7 which were induced from human dermal fibroblasts by the transfection of OCT3/4, SOX2, KLF4 and c-MYC [16] and 253G1 which were induced from human dermal fibroblasts by the transfection of OCT3/4, SOX2 and KLF4 [10]. Cell culture of iPSCs was according to previously described methods [12,15,16].

Differentiation of iPSCs by serum-free embryoid body-like (SFEB) culture was performed according to previously described method [6,13,18]. Briefly, 5×10^4 cells/ml of iPSCs were cultured in 100 mm low cell binding dishes (Nalge NUNC international, Rochester, NY) with ES differentiation medium [G-MEM (GIBCO) containing 5% KSR, 0.1 mM nonessential amino acids, 1 mM sodium pyruvate, 0.1 mM 2-mercaptoethanol, 50 units/ml penicillin, and 50 μg/ml streptomycin]. Recombinant Dkk-1, a Wnt antagonist, (100 ng/ml, R&D Systems, Minneapolis, MN) and recombinant Lefty A, a Nodal antagonist (500 ng/ml, R&D Systems) were added to the medium during the suspension culture. Floating cells that formed aggregates were plated on poly-D-lysine, laminin and fibronectin-coated slides. Cells were then harvested for subsequent analysis. To compare mouse ES and iPS cells, the mouse ES cell line RF8 was maintained and differentiated in cultures identical to those described above. After determining the method for induction of $Rx^+/Pax6^+$ retinal progenitors, the duration of adherent culture

* Corresponding author. Tel.: +81 78 306 3301; fax: +81 78 306 3303.
E-mail address: mretina@cdb.riken.jp (M. Takahashi).

0304-3940/$ – see front matter © 2009 Elsevier Ireland Ltd. All rights reserved.
doi:10.1016/j.neulet.2009.04.035

was extended to generate retinal photoreceptor cells. SFEB/DL-treated differentiated cells were incubated in the RA/T medium [13] [G-MEM containing 5% KSR, N2 supplement (GIBCO), retinoic acid (1 μM, Sigma), taurine (100 μM, Sigma), 0.1 mM nonessential amino acids, 1 mM sodium pyruvate, 0.1 mM 2-mercaptoethanol, 50 units/ml penicillin, and 50 μg/ml streptomycin].

For directed differentiation, human iPS colonies were partially dissociated into clumps (5–10 cells/clump) by treatment with 0.25% trypsin and 0.1 mg/ml collagenase IV in PBS containing 1 mM $CaCl_2$ and 20% KSR, followed by gentle trituration. Feeders were removed by incubation of the iPS clumps on a gelatin-coated dish. Human iPS clumps, at a density of 6.7×10^2 clumps/ml, were incubated in a 100 mm low cell binding dish in human ES medium for 2 days, in 20% KSR-containing ES differentiation medium (G-MEM, 0.1 mM nonessential amino acids, 1 mM pyruvate and 0.1 mM 2-mercaptoethanol) for 4 days, then in 15% KSR-containing ES differentiation medium for 8 days, and subsequently in 10% KSR-containing ES differentiation medium for 6 days. Dkk-1 (100 ng/ml) and Lefty A (500 ng/ml) were applied to the medium for 20 days while in suspension culture. Human iPS cell aggregates were then replated en bloc on poly-D-lysine/laminin/fibronectin-coated 8-well culture slides at a density of 10–15 aggregates/cm^2. In adherent

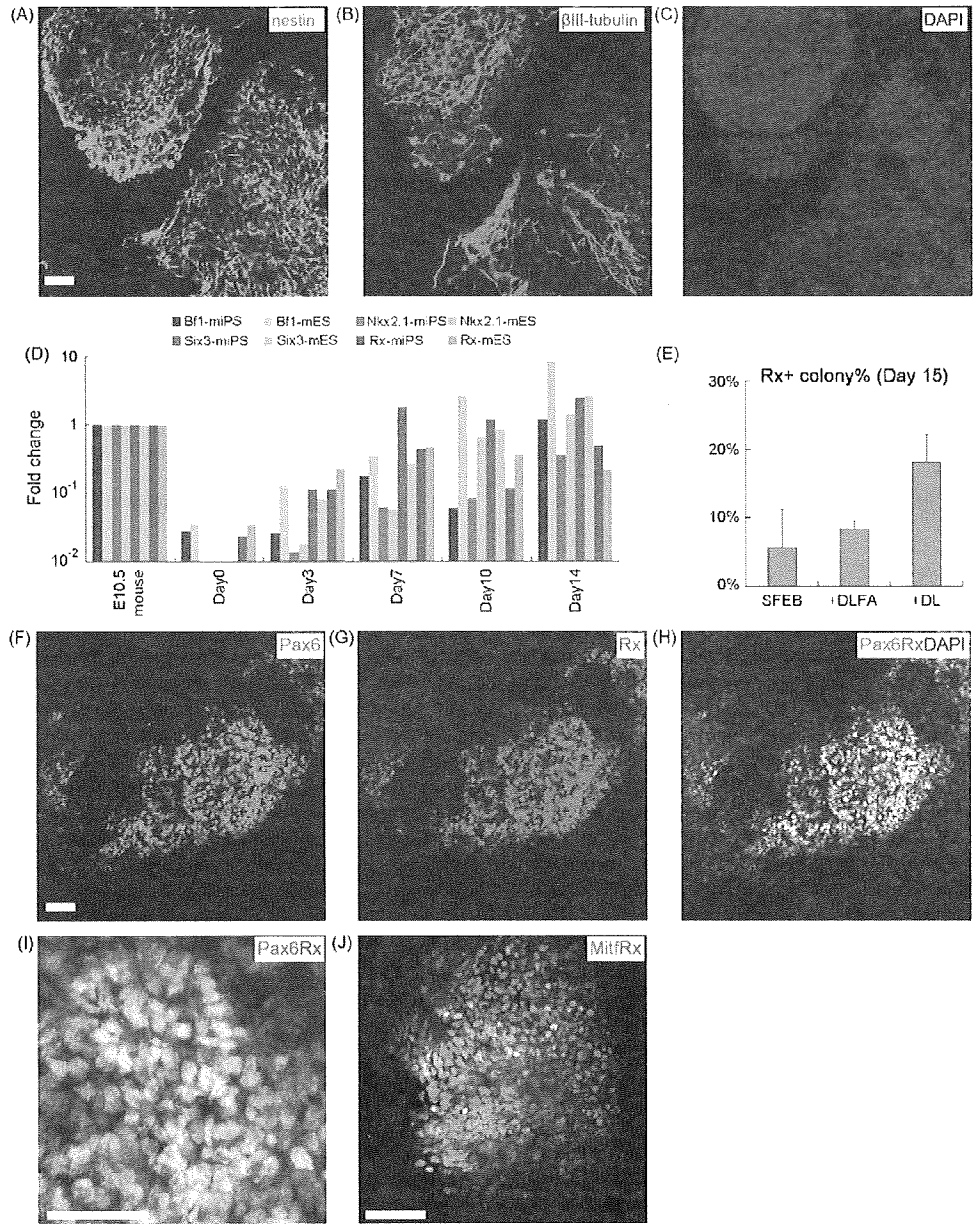

Fig. 1. Directed differentiation of neural and retinal progenitors from mouse induced pluripotent stem (iPS) cells. (A–C) Immunostaining of mouse iPSCs in SFEB conditions with anti-nestin and anti-βIII-tubulin antibodies on day 9. Cell nuclei were counterstained with 4′,6-diamidino-2-phenylindole (DAPI). (D) Fold change of the gene expression by real-time RT-PCR analysis of the neural markers *Bf1* and *Nkx2.1*, the eye field marker *Six3* and the retinal progenitor marker *Rx* in mouse iPSCs under SFEB culture conditions (reference; head portion of mouse embryo [E10.5]). (E) The percentage of $Rx^+/Pax6^+$ colonies in different culture conditions of mouse iPSCs on day 15. SFEB: a serum-free, feeder-free suspension culture. SFEB/DLFA: the SFEB culture combined with Dkk-1 (100 ng/ml) and the Lefty A (500 ng/ml) on day 0, FBS (5%) on day 4, and Activin A (100 ng/ml) on day 5. SFEB/DL: the SFEB culture combined with Dkk-1 (100 ng/ml) and the Lefty A (500 ng/ml) from day 0 to 9. (F–H) Immunostaining of mouse iPSCs in SFEB/DL conditions with anti-Rx and anti-Pax6 antibodies on day 15. (I) Magnified view of $Rx^+/Pax6^+$ cells in mouse iPSCs under SFEB/DL conditions on day 15. (J) Immunostaining of mouse iPSCs in SFEB/DL conditions with anti-Mitf and anti-Rx antibodies on day 15. Scale bars; 50 μm.

cultures, cells were incubated in 10% KSR-containing ES differentiation medium. For photoreceptor differentiation, human iPSCs were incubated under SFEB/DL conditions for 90 days, and subsequently in RA/T medium for at least 30 days. The medium was changed every day.

Total RNA was extracted from cultured iPSCs with TRIzol reagent (Invitrogen). Complementary DNA was then synthesized from RNA with a first-strand cDNA synthesis kit (GE Healthcare Bio-Sciences, Piscataway, NJ). The synthesized cDNA from each sample was amplified with Power SYBR Green PCR Master Mix (Applied Biosystems, Foster City, CA) using gene-specific primers in a step cycle program for 40 cycles under the following conditions: denaturation at 95 °C for 15 s, annealing at 60 °C for 60 s. Primers used for RT-PCR analyses were listed in supplementary methods. Data normalization was performed in reference to the gene expression level of the head portion of mouse E10.5 embryo in neural and retinal progenitor marker genes (*Bf1*, *Nkx2.1*, *Six3*, *Rx*), undifferentiated iPSCs in undifferentiated cell marker genes (*Oct3/4*, *Nanog*) or the neonatal mouse retina in photoreceptor marker genes (*Crx*).

Immunocytochemistry was performed as described previously [13]. Briefly, cultured iPSCs were fixed with 4% paraformaldehyde for 15 min at 25 °C, washed with phosphate buffered saline (PBS) and blocked with 5% goat serum and 0.3% Triton X-100 (Sigma) in PBS. The samples were incubated overnight at 4 °C with primary antibodies and 0.3% Triton X-100. After primary antibodies were removed and the samples were washed, secondary antibodies were applied for 1 h at 25 °C. Primary and secondary antibodies were listed in supplementary methods. Cell nuclei were counterstained with 4′,6-diamidino-2-phenylindole (DAPI; 1 μg/ml, molecular probes—Invitrogen). Labeled cells were imaged with a confocal laser scanning microscope (Radiance 2100; Bio-Rad Laboratories, Hercules, CA).

Undifferentiated and SFEB/DL-treated iPS cell aggregates were dissociated as previously described [6]. The aggregates were suspended with 0.25% trypsin/EDTA (Invitrogen) and DNase I (10 μg/ml, Sigma) into single cells. After neutralization of trypsin with DMEM containing 10% FBS, the cells were resuspended in HBSS containing 0.1% BSA and 5 μg/ml propidium iodide (Sigma), and passed through a cell strainer (BD, Franklin Lakes, NJ). Cells were counted by FACS Aria (BD Biosciences), and the data were analyzed with FACS Diva software (BD Biosciences). Dead cells were excluded by gating forward and side scatter as well as by PI staining.

Data are expressed as means ± S.E.M. The reproducibility of the results was confirmed in at least three independent sets of experiments. The statistical significance of difference was evaluated with an unpaired *t*-test or with one-way analysis of variance (ANOVA) followed by Dunnett's test. Probability values less than 5% were considered significant.

A published study has reported that mouse ES cells can be efficiently differentiated into neural progenitors in a serum-free, feeder-free suspension culture (SFEB) [18]. In addition, retinal progenitors can be induced by combining soluble factors with the SFEB method [6,13]. To induce differentiation of mouse iPSCs with the SFEB method, mouse iPSCs (iPS-MEF-Ng-20D-17) [12] were seeded in Petri dishes as suspension cultures. After 6 days of floating culture, the aggregates were adhered onto glass slides coated with poly-D-lysine, laminin, and fibronectin, and cultured for another 3 days (day 9). Immunocytochemical analysis revealed that nearly all of the aggregates expressed nestin (99.3 ± 0.65% of total colonies) and βIII-tubulin (98.0 ± 1.1% of total colonies) (Fig. 1A–C). Since Wnt and TGFβ signals have negative effects on mammalian neural differentiation [1,14], we applied the Wnt antagonist Dkk-1 (100 ng/ml) and the Nodal antagonist Lefty A (500 ng/ml) during suspension culture (SFEB/DL method) [18]. According to the method which was previously reported with mouse ES cells [6], fetal bovine serum (FBS; Invitrogen) was added in the medium with 5% at the final concentration on day 4, and Activin A (100 ng/ml; R&D) was added in the medium on day 5 (SFEB/DLFA method). Floating aggregates were plated on coated slides. Cells were fixed on day 9 and used for subsequent immunocytochemical analysis. However, we could not detect cells positive for the retinal progenitor markers Rx, Pax6 and Mitf. We then prolonged the duration of adhesion culture period and examined the mRNA expression of central nervous system (CNS) region-specific markers by real-time PCR. The expression of telencephalic markers *Bf1*, *Nkx2.1* and *Six3* and the eye field marker *Rx* in iPSCs were found to be increased after inducing differentiation by the SFEB/DL method. This observation is similar to the differentiation of ES cells (Fig. 1D). Mouse iPSCs were cultured under the SFEB conditions and probed for the retinal progenitor markers Rx, Pax6 and Mitf. On day 15, we observed 18.1 ± 4.1% of total colonies double positive for both Rx and Pax6 under the SFEB/DL conditions (5.56 ± 5.6% under the SFEB conditions and 8.26 ± 1.2% under the SFEB/DLFA conditions) (Fig. 1E–I). The SFEB/DL method tends to increase the number of Rx^+ cells than the SFEB method, although there was no statistical significant difference between them. Under SFEB/DL conditions, 22.3 ± 3.9% of cells was Rx^+ within the positive colonies. In addition, 36.2 ± 5.1% of total colonies cultured under SFEB/DL conditions also expressed Mitf, a marker of RPE progenitors (11.4 ± 3.4% of cells in those colonies; Fig. 1J). The $Mitf^+$ cells and Rx^+ cells were frequently found in the same clusters. We conclude from these results that mouse iPSCs differentiate into retinal progenitors following SFEB/DL-treatment.

Second, we assessed the number of undifferentiated cells during differentiation. Mouse Nanog-iPS cells express GFP protein with Nanog [12]. Under conditions that did not induce differentiation, 96.2 ± 0.10% of total cells was positive for Nanog-GFP by flow cytometry (Fig. 2A). In contrast, the level of fluorescence of Nanog-GFP significantly decreased in iPSCs as the SFEB or SFEB/DL culture progressed. At day 8 and day 15, 4.05 ± 0.62% and 0.60 ± 0.04% of cells were Nanog-GFP^+, respectively (Fig. 2B and C). Thus, a small number of cells remained undifferentiated even after 15 days. Real-time PCR analysis also revealed that expression of markers for undifferentiated cells Oct3/4 and Nanog gradually decreased over the period of differentiation (Fig. 2D). This finding parallels our observation with mouse ES cells cultured under identical conditions (data not shown).

Third, we examined the differentiation potential of retinal progenitors derived from mouse iPSCs. RPE cells form tight junctions

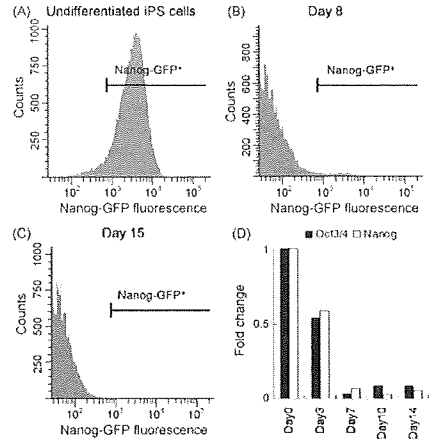

Fig. 2. The analysis of residual undifferentiated mouse iPSCs under SFEB/DL conditions. (A–C) The number of residual undifferentiated iPSCs present after differentiation was determined by flow cytometry of Nanog-GFP positive undifferentiated iPSCs on days 8 and 15 under SFEB/DL conditions. (D) Fold change of the gene expression by RT-PCR analysis of the undifferentiated cell markers *Oct3/4* and *Nanog* in mouse iPSCs under SFEB/DL conditions (reference; undifferentiated mouse iPSCs).

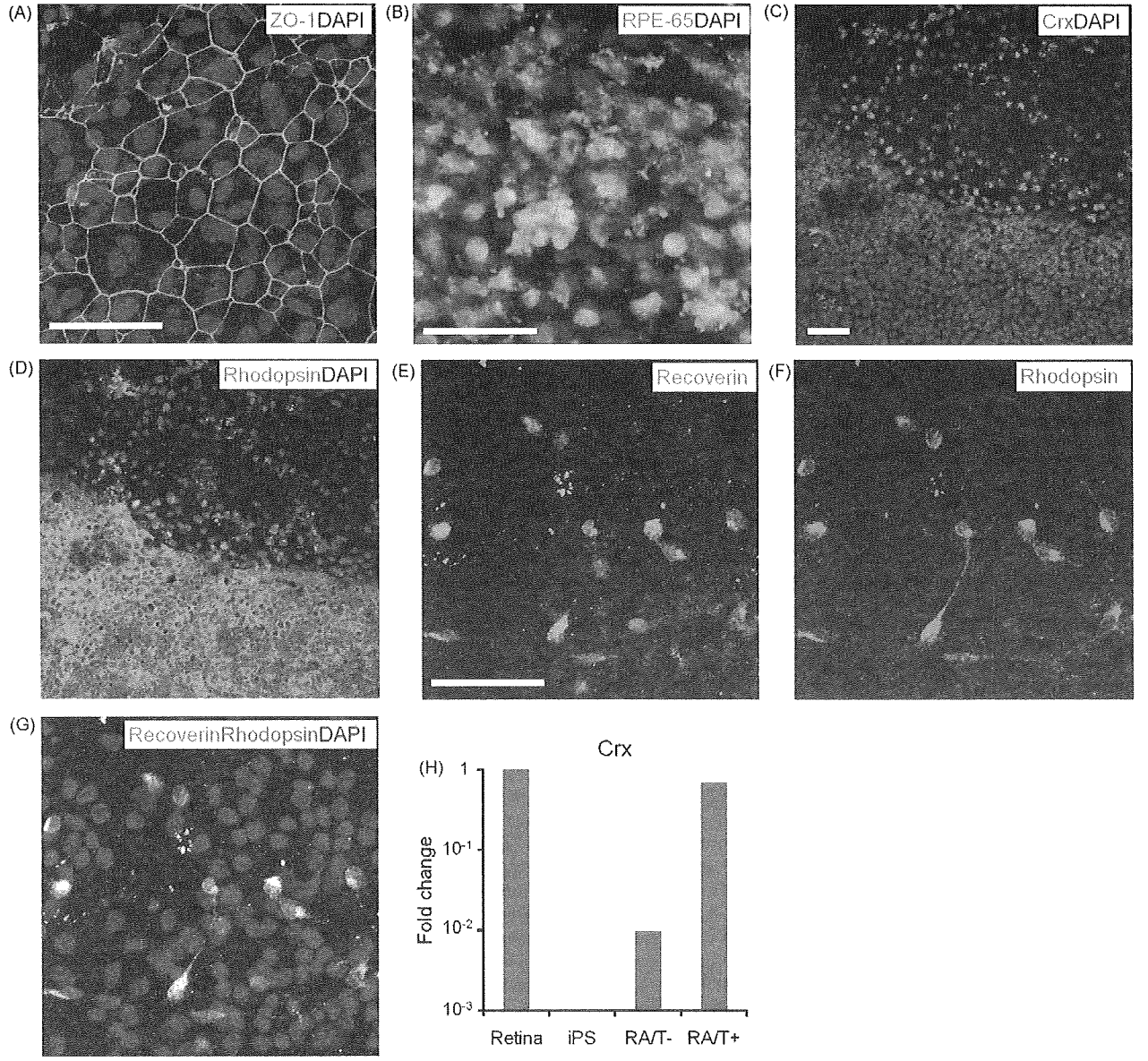

Fig. 3. Differentiation of mouse iPSCs into putative retinal pigment epithelium and photoreceptors. (A) Staining of tight junctions with an anti-ZO-1 antibody in mouse iPSCs under SFEB/DL conditions on day 30. (B) Immunostaining of mouse iPSCs with anti-RPE65 antibodies on day 45 in SFEB/DL conditions. (C and D) Immunostaining of mouse iPSCs with anti-Crx and anti-rhodopsin antibodies on day 45 in SFEB/DL conditions following the application of retinoic acid (1 μM) and taurine (100 μM). (E–G) Immunostaining of mouse iPSCs with anti-recoverin and anti-rhodopsin antibodies on day 45 in SFEB/DL conditions following the application of retinoic acid (1 μM) and taurine (100 μM). (H) Fold change of the gene expression by RT-PCR analysis of the photoreceptor marker *Crx* in mouse iPSCs under SFEB/DL conditions with or without retinoic acid and taurine treatment on day 45 (reference; neonatal mouse retina). Scale bars: 50 μm.

with hexagonal morphology *in vivo*. Therefore, we determined the expression of ZO-1, a tight junction marker. On day 30, ZO-1 was expressed at the lateral border of polygonal-shaped cells cultured under SFEB/DL culture conditions (Fig. 3A). We also found cells positive for a RPE specific marker, RPE-65 on day 45 (Fig. 3B). Next, according to the differentiation method for ES cells [13], we treated mouse iPSCs differentiated with the SFEB/DL method with retinoic acid (1 μM) and taurine (100 μM), both of which are important for photoreceptor genesis [8], beginning at differentiation day 24 (RA/T treatment). On day 45, we observed cells that were immunopositive for both the photoreceptor precursor marker Crx and the mature rod photoreceptor marker rhodopsin (Fig. 3C and D). The rhodopsin$^+$ cells co-expressed another photoreceptor marker, recoverin (Fig. 3E–G). Real-time PCR analysis showed fold increase of Crx expression in differentiated mouse iPSCs with RA/T treatment than in those without RA/T treatment (Fig. 3H). Thus, we conclude that induced retinal progenitors have competence to differentiate into putative photoreceptors and RPE cells.

Finally, we examined whether human iPSCs could differentiate into retinal progenitors when treated with a method similar to that used for human ES cells. Human iPSCs (201B6, 201B7 and 253G1) [16,10] were dissociated into small clumps of 5–10 cells and seeded in Petri dishes as suspension cultures with serum-free medium containing Dkk-1 (100 ng/ml) and Lefty A (500 ng/ml). Under these conditions, human iPSCs formed embryoid body-like aggregates. On day 20, aggregates were plated onto glass slides coated with poly-D-lysine, laminin, and fibronectin. On day 35, we observed marked expression of the neural differentiation marker nestin and

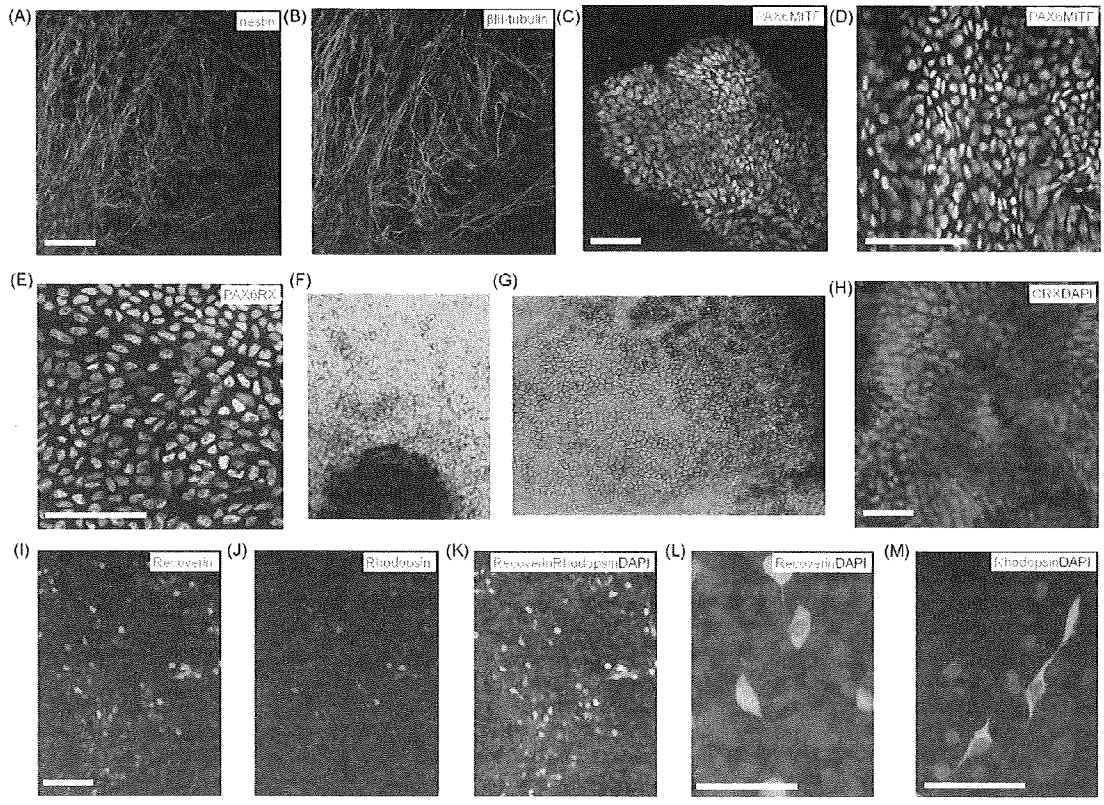

Fig. 4. Directed differentiation of neural and retinal progenitors and induction of photoreceptor properties from human induced pluripotent stem (iPS) cells. (A and B) Immunostaining of human iPSCs in SFEB/DL conditions with anti-nestin and anti-βIII-tubulin antibodies on day 35. (C and D) Presumptive RPE cells immunopositive for anti-Mitf and anti-Pax6 antibodies in human iPS cell cultures in SFEB/DL conditions on day 35. (E) Retinal progenitor cells immunopositive for anti-Rx and anti-Pax6 antibodies in human iPS cell cultures in SFEB/DL conditions on day 35. (F and G) Pigmented cells in human iPS cell cultures in SFEB/DL conditions display RPE-like polygonal morphologies on day 60. (H) Immunostaining of human iPSCs in SFEB/DL conditions with anti-Crx antibody on day 80. (I–M) Immunostaining of human iPSCs with anti-recoverin and anti-rhodopsin antibodies on day 120 in SFEB/DL conditions following the application of retinoic acid (1 μM) and taurine (100 μM). Scale bars: 50 μm.

βIII-tubulin (Fig. 4A and B). Under SFEB/DL conditions, 29.8 ± 4.0% of total colonies of these differentiated iPSCs were $MITF^+/PAX6^+$ (Fig. 4C and D) and 19.4 ± 4.9% were $RX^+/PAX6^+$ (Fig. 4E). These results mirror our results with human ES cells [13]. The $MITF^+$ cells were frequently found in close proximity to RX^+ cells. Thus, human iPSCs can be differentiated into retinal progenitors. On day 40, pigmented cells were evident under the light microscopy in the SFEB/DL cultures (38.8 ± 6.8% of total colonies). We could observe these differentiated cells in two human iPS cell lines 201B7 and 253G1; however, pigmented cells, $MITF^+/PAX6^+$ or $RX^+/PAX6^+$ cells were not detected in an iPS cell line 201B6 with the same differentiation method. We then used the cell lines 201B7 and 253G1 for further analyses. Over time, these cells adopted a polygonal morphology, a characteristic of RPE cells (Fig. 4F and G). On day 80, 14.1 ± 5.5% of total colonies were positive for CRX, a photoreceptor precursor maker (Fig. 4H). To determine the potential for human iPSCs to express photoreceptor properties, we treated these cells with SFEB/DL, and subsequently with retinoic acid (1 μM) and taurine (100 μM), beginning at differentiation day 90. On day 120, we observed that 26.5 ± 8.3% of total colonies and 13.2 ± 1.6% of cells in those colonies were immunopositive for the photoreceptor marker recoverin. We also observed 49.9 ± 9.8% of recoverin positive cells co-expressed the rod photoreceptor marker rhodopsin (Fig. 4I–M). Taking together, we conclude that human iPSCs differentiate toward retinal fates with the differentiation method for human ES cells.

In this study, we have demonstrated that mouse and human iPSCs can be induced with defined factors to differentiate *in vitro* into retinal progenitors. Serum-free embryoid body-like cultures were used to induce neural differentiation of mouse and human iPSCs. Following treatment with Wnt and Nodal inhibitors, retinal progenitors positive for Rx, Pax6 and Mitf were evident. Subsequently, morphologically mature RPE-like cells were observed. Application of retinoic acid and taurine induced these cells to express the retinal photoreceptor markers Crx, recoverin, and rhodopsin. We conclude from this progression of the marker expression that these iPSCs differentiated into retinal progenitors and then putative photoreceptor and RPE cells. These differentiation conditions are the same that induced retinal progenitors, RPE and photoreceptors from ES cells [13].

In mouse ES cell cultures, we previously showed that $Rx^+/Pax6^+$ cells were observed on day 9 after differentiation was started. In this study with mouse iPS cell cultures, we could observe $Rx^+/Pax6^+$ cells not on day 9, but on day 15. The explanation for this result was not clear, but might have some relation to the condition of maintenance of mouse ES and iPS cells. The mouse ES cell line used in our previous study (EB5) was maintained in feeder-free, low concentration of FBS (5%) medium condition and appeared epithelia-like morphology. Although the cell line was selected by antibiotics resistant gene expression together with the expression of a pluripotent cell marker Oct3/4, the cell line may have a tendency of differentiation into ectoderm or neural lineage. The mouse iPS and ES cell lines (iPS-20D17 and RF8) that we used in this study were maintained with SNL feeder cells and in the medium containing 15% FBS, might take more time to neural and retinal differentiation.

We also previously showed that, in mouse ES cell cultures, DAPT, a Notch inhibitor, promotes photoreceptor differentiation in FACS-purified Rx^+ cells, although it has little effect on Rx^+ cells present in unpurified SFEB-treated cells. DAPT was not used in this study

because we considered that, similar to our previous study, DAPT would not effective on photoreceptor differentiation of mouse iPSCs without purification of Rx^+ cells.

In our differentiation condition, the differentiation efficiency of RPE and photoreceptors from human iPS cell cultures with cell lines 201B7 and 253G1 was not different from that human ES cell cultures. Therefore, in addition to their similarity in pluripotency, retinal differentiation methods using defined factors for ES cells are also applicable to iPSCs, although further research will be required to characterize the function of induced retinal cells.

The clinical applications for transplantation of cells cultured with materials from other animals, such as feeder cells or serum, are hampered by the risk of adverse immunologic response and potential exposure to xeno-pathogens. Thus, it is important to develop culture methods with defined factors that are free of animal-derived materials for the differentiation *in vitro* of cells required for transplantation. In the present study, we have succeeded in *in vitro* differentiation of both mouse and human iPSCs with the serum-free, feeder-free method, but the culture technique still includes animal-derived products such as KSR, N2 supplement, culture matrix and dissociation solutions. And it is also true that the production of iPS cell lines requires serum, KSR and feeder cells. Thus, we need to establish a xeno-free culture method for clinical application of iPSCs in cell transplantation therapy.

As for immune rejection, transplantation of patient-specific cells will have several advantages over comparable differentiated ES cells [10]. In exudative age-related macular degeneration, a retinal disease which causes severe visual deficits as a consequence of the patchy loss of RPE and disruption of the RPE-photoreceptor interface by the ingrowing subretinal fibrovascular tissue, introducing healthy RPE under the fovea and repair of Bruch's membrane may promote significant recovery of vision when performed in conjunction with surgical removal of subretinal fibrovascular tissue. However, allogenic RPE transplantation is likely to induce rejection of graft tissue in the absence of systemic immunosuppression [17]. Moreover, macular translocation surgery or autologous RPE and choroid patch translocation include a risk of serious surgical complications [7]. Therefore, transplantation of RPE cells derived from patient-specific iPSCs will have prominent advantages.

However, a risk of tumor formation by contaminating undifferentiated cells is not resolved [3]. Indeed, at least 0.6% of the mouse iPSCs remained undifferentiated in our cultures even 15 days after differentiation. Thus, to prevent tumor formation, establishment of purification methods will be requisite.

In summary, we demonstrated that iPSCs can differentiate into retinal-like cells with defined factors *in vitro* when induced with the same methodology used to differentiate ES cells. Future studies will be required to determine whether putative RPE and photoreceptors differentiated from iPSCs restore visual function when transplanted into the degenerative retina. Optimizing the differentiation of iPSCs and transplantation methods will facilitate the development of transplantation therapies for retinal diseases.

Acknowledgements

We thank Y. Sasai (RIKEN) for kindly providing Rx and Crx antibodies, A. Nomori, K. Iseki and C. Ishigami for technical assistance and the members of Takahashi laboratory for discussions. This work was supported by Grants-in-Aid from the Ministry of Education, Culture, Sports, Science and Technology of Japan (Y.H. and M.T.), the Mochida Memorial Foundation for Medical and Pharmaceutical Research (F.O.), and the Leading Project (M.T.)

Appendix A. Supplementary data

Supplementary data associated with this article can be found, in the online version, at doi:10.1016/j.neulet.2009.04.035.

References

[1] J. Aubert, H. Dunstan, I. Chambers, A. Smith, Functional gene screening in embryonic stem cells implicates Wnt antagonism in neural differentiation, Nat. Biotechnol. 20 (2002) 1240–1245.
[2] S. Chen, Q.L. Wang, Z. Nie, H. Sun, G. Lennon, N.G. Copeland, D.J. Gilbert, N.A. Jenkins, D.J. Zack, Crx, a novel Otx-like paired-homeodomain protein, binds to and transactivates photoreceptor cell-specific genes, Neuron 19 (1997) 1017–1030.
[3] H. Fukuda, J. Takahashi, K. Watanabe, H. Hayashi, A. Morizane, M. Koyanagi, Y. Sasai, N. Hashimoto, Fluorescence-activated cell sorting-based purification of embryonic stem cell-derived neural precursors averts tumor formation after transplantation, Stem Cells 24 (2006) 763–771.
[4] T. Furukawa, C.A. Kozak, C.L. Cepko, Rax, a novel paired-type homeobox gene, shows expression in the anterior neural fold and developing retina, Proc. Natl. Acad. Sci. U.S.A. 94 (1997) 3088–3093.
[5] T. Furukawa, E.M. Morrow, C.L. Cepko, Crx, a novel otx-like homeobox gene, shows photoreceptor-specific expression and regulates photoreceptor differentiation, Cell 91 (1997) 531–541.
[6] H. Ikeda, F. Osakada, K. Watanabe, K. Mizuseki, T. Haraguchi, H. Miyoshi, D. Kamiya, Y. Honda, N. Sasai, N. Yoshimura, M. Takahashi, Y. Sasai, Generation of $Rx^+/Pax6^+$ neural retinal precursors from embryonic stem cells, Proc. Natl. Acad. Sci. U.S.A. 102 (2005) 11331–11336.
[7] A.M. Joussen, F.M. Heussen, S. Joeres, H. Llacer, B. Prinz, K. Rohrschneider, K.J. Maaijwee, J. van Meurs, B. Kirchhof, Autologous translocation of the choroid and retinal pigment epithelium in age-related macular degeneration, Am. J. Ophthalmol. 142 (2006) 17–30.
[8] E.M. Levine, S. Fuhrmann, T.A. Reh, Soluble factors and the development of rod photoreceptors, Cell. Mol. Life. Sci. 57 (2000) 224–234.
[9] P.H. Mathers, A. Grinberg, K.A. Mahon, M. Jamrich, The Rx homeobox gene is essential for vertebrate eye development, Nature 387 (1997) 603–607.
[10] M. Nakagawa, M. Koyanagi, K. Tanabe, K. Takahashi, T. Ichisaka, T. Aoi, K. Okita, Y. Mochiduki, N. Takizawa, S. Yamanaka, Generation of induced pluripotent stem cells without Myc from mouse and human fibroblasts, Nat. Biotechnol. 26 (2007) 101–106.
[11] M. Nguyen, H. Arnheiter, Signaling and transcriptional regulation in early mammalian eye development: a link between FGF and MITF, Development 127 (2000) 3581–3591.
[12] K. Okita, T. Ichisaka, S. Yamanaka, Generation of germline-competent induced pluripotent stem cells, Nature 448 (2007) 313–317.
[13] F. Osakada, H. Ikeda, M. Mandai, T. Wataya, K. Watanabe, N. Yoshimura, A. Akaike, Y. Sasai, M. Takahashi, Toward the generation of rod and cone photoreceptors from mouse, monkey and human embryonic stem cells, Nat. Biotechnol. 26 (2008) 215–224.
[14] S. Parisi, D. D'Andrea, C.T. Lago, E.D. Adamson, M.G. Persico, G. Minchiotti, Nodal-dependent Cripto signaling promotes cardiomyogenesis and redirects the neural fate of embryonic stem cells, J. Cell Biol. 163 (2003) 303–314.
[15] K. Takahashi, S. Yamanaka, Induction of pluripotent stem cells from mouse embryonic and adult fibroblast cultures by defined factors, Cell 126 (2006) 663–676.
[16] K. Takahashi, K. Tanabe, M. Ohnuki, M. Narita, T. Ichisaka, K. Tomoda, S. Yamanaka, Induction of pluripotent stem cells from adult human fibroblasts by defined factors, Cell 131 (2007) 861–872.
[17] T.H. Tezel, L.V. Del Priore, A.S. Berger, H.J. Kaplan, Adult retinal pigment epithelial transplantation in exudative age-related macular degeneration, Am. J. Ophthalmol. 143 (2007) 584–595.
[18] K. Watanabe, D. Kamiya, A. Nishiyama, T. Katayama, S. Nozaki, H. Kawasaki, Y. Watanabe, K. Mizuseki, Y. Sasai, Directed differentiation of telencephalic precursors from embryonic stem cells, Nat. Neurosci. 8 (2005) 288–296.

Osteoarthritis and Cartilage (2009) **17,** 529–538

doi:10.1016/j.joca.2008.09.003

Osteoarthritis and Cartilage | ICRS International Cartilage Repair Society | OA OSTEOARTHRITIS

PGE2 signal *via* EP2 receptors evoked by a selective agonist enhances regeneration of injured articular cartilage

S. Otsuka M.D.†‡, T. Aoyama M.D., Ph.D.†*, M. Furu M.D.†§, K. Ito M.D.†‡, Y. Jin M.D.†, A. Nasu M.D.†§, K. Fukiage M.D.†§, Y. Kohno M.D., Ph.D.†§, T. Maruyama Ph.D.‖, T. Kanaji‖, A. Nishiura Ph.D.‖, H. Sugihara‖, S. Fujimura‖, T. Otsuka M.D., Ph.D.‡, T. Nakamura M.D., Ph.D.§ and J. Toguchida M.D., Ph.D.†

† *Department of Tissue Regeneration, Institute for Frontier Medical Sciences, Kyoto University, Kyoto, Japan*
‡ *Department of Orthopaedic Surgery, Graduate School of Medical Sciences, Nagoya City University, Nagoya, Japan*
§ *Department of Orthopaedic Surgery, Graduate School of Medicine, Kyoto University, Kyoto, Japan*
‖ *Ono Pharmaceutical Co. Ltd., Osaka, Japan*

Summary

Objective: The effect of the prostaglandin E2 (PGE2) signal through prostaglandin E receptor 2 (EP2) receptors on the repair of injured articular cartilage was investigated using a selective agonist for EP2.

Methods: Chondral and osteochondral defects were prepared on the rabbit femoral concave in both knee joints, and gelatin containing poly-lactic-co-glycolic acid microspheres conjugated with or without the EP2 agonist was placed nearby. Animals were sacrificed at 4 or 12 weeks post-operation, and regenerated cartilage tissues and subchondral structure remodeling were evaluated by histological scoring. The quality of regenerated tissues was also evaluated by the immunohistochemical staining of EP2, type II collagen, and proliferating cell nuclear antigen (PCNA). As an evaluation of side effects, the inflammatory reaction of the synovial membrane was analyzed based on histology and the mRNA expression of matrix metalloproteinase3 (MMP3), tissue inhibitor of metalloproteinase 3 (TIMP3), and interleukin-1β (IL-1β). Also, the activity of MMP3 and the amount of tumor necrosis factor-α (TNF-α) and C-reactive protein in joint fluid were measured.

Results: In both models, the EP2 agonist enhanced the regeneration of the type II collagen-positive tissues containing EP2- and PCNA-positive chondrocytes, and the histological scale of regenerated tissue and subchondral bone was better than that of on the control side, particularly at 12 weeks post-operation. No inflammatory reaction in the synovial membrane was observed, and no induction of pro-inflammatory cytokines was found in joint fluid.

Conclusion: Selective stimulation of the PGE2 signal through EP2 receptors by a specific agonist promoted regeneration of cartilage tissues with a physiological osteochondral boundary, suggesting the potential usefulness of this small molecule for the treatment of injured articular cartilages.

Key words: PGE2, EP2, Agonist, Cartilage, Defect, Repair, Therapeutic drug, Osteoarthritis.

Introduction

Chondrocytes in articular cartilage are differentiated cells with minimum proliferating potential and low metabolic activity[1]. Because these cells are fully responsible for the production of cartilage matrix consisting of collagens and proteoglycans, considerable damage to articular cartilage is unrepairable, initiating a sequence of catabolic events leading to a pathological condition known as osteoarthritis (OA). Although inflammation of the synovium and the destruction of subchondral bone integrity also play an important role in the progression of OA, the poor regenerative capacity of chondrocytes is the major disease-causing factor[1,2]. In the early stages of OA, however, not only catabolic but also anabolic activity is enhanced in chondrocytes. As catabolic activity, chondrocytes produce several catabolic cytokines such as interleukin-1 (IL-1), which in turn induce the production of proteinases such as matrix metalloproteinases (MMPs) and a disintegrin-like and metalloprotease with thrombospondin (ADAMTS) leading to the destruction of the matrix network[2]. As anabolic activity, chondrocytes produce anabolic cytokines such as the bone morphogenic protein (BMP) family and insulin like growth factor-1 (IGF-1), which induce the synthesis of collagens and initiate the proliferation of chondrocytes themselves making osteophytes at the periphery[2]. A disruption of the equilibrium between the catabolic and anabolic activities results in catastrophic damage to articular cartilage. In adult articular cartilage, the equilibrium leans toward catabolic activity; the proliferation of chondrocytes is decreased and the subchondral structure is weak.

The role of prostaglandin E2 (PGE2) in the development of OA is controversial. Pro-inflammatory signal mediators such as IL-1 and tumor necrosis factor-α (TNF-α) induce

*Address correspondence and reprint requests to: Dr T. Aoyama, M.D., Ph.D., Department of Tissue Regeneration, Institute for Frontier Medical Sciences, Kyoto University, 53 Kawahara-cho, Shogoin, Sakyo-ku, Kyoto 606-8507, Japan. Tel: 81-75-751-4107; Fax: 81-75-751-4646; E-mail: blue@frontier.kyoto-u.ac.jp
Received 13 April 2008; revision accepted 2 September 2008.

the synthesis of PGE2 by promoting the expression or activities of cycloxygenase (COX)-2 and microsomal PGE synthase-1[3]. The synthesized PGE2 promotes IL-1 expression as a positive feedback mechanism, degrades the cartilage matrix[4], and finally induces apoptosis of chondrocytes[5], indicating a catabolic role for PGE2 in OA. In some reports, however, anabolic effects of PGE2 were demonstrated[1,3]. PGE2 opposed the effect of IL-1 by down-regulating type I collagen[6] and stimulating type II collagen gene expression[7,8]. Also, PGE2 stimulated the synthesis of proteoglycan and collagen through the induction of IGF-1-binding protein[9], and induced the proliferation of rat chondrocytes as demonstrated by an increase in the incorporation of [^{3}H]-thymidine[9].

Several factors are involved in these controversial findings including experimental design, the level of PGE2 expression, the balance with other pro-inflammatory cytokines, and most notably, the variety of receptors. PGE2 exerts its biological effect through one of four receptors, EP1, EP2, EP3, or EP4. The development of specific agonists and antagonist for each receptor enables the understanding of the receptor-specific signal transduction mechanism and its consequence. Signals through EP1 and EP3 coupled by G_i protein increase the intra-cellular Ca^{2+} concentration, and those through EP2 and EP4 coupled by G_s protein increase cyclic adenosine monophosphate (cAMP). Although the second messenger is common, the amide acid identity is only 31% between EP2 and EP4. EP4 (513 amino acids) has the longest intra-cellular C terminal, but EP2 (362 amino acids) has a compact structure. In osteoclastogenesis, the EP2 and EP4 mediate the induction of receptor activator of nuclear factor-kappa B (NF-κB) ligand (RANKL), but the extent of the contribution by each receptor is different. Although both EP2 and EP4 are expressed in dendritic cell, EP4 has selective action for cell migration. This selectivity of EP4 may be caused by the fact that EP4 but not EP2 couples to phosophatidylinositol 3-kinase in addition to cAMP[10].

We have previously demonstrated that EP2 was the major PGE2 receptor in articular chondrocytes[11]. And a specific agonist for EP2 not EP4 promoted the growth of mouse and human chondrocytes by up-regulating the expression of growth-promoting genes such as the *cyclin D* gene stimulating the increase of cAMP[11]. The protein structure and function of EP2 are conserved between many species, and the amino acid homology between the human and mouse, rat, or rabbit is 88.2, 84.9, and 90.2%, respectively. The effect of the EP2 agonist on chondrocytes was confirmed in a rat organ culture system, suggesting the possible application of this small molecule as a new therapeutic tool for injured articular cartilage[11].

In this study, we investigated the effect of an EP2 agonist on injured articular cartilage *in vivo* using rabbit knee joints and also on other joint structures such as the synovium and subchondral bone.

Materials and methods

REAGENTS

Microspheres loaded with the selective EP2 agonist, ONO-8815Ly[12] prepared by the emulsion–solvent evaporation method as described[13]. Briefly, ONO-8815Ly was dissolved in purified water as the inner water phase and polylactic-co-glycolic acid (PLGA) was dissolved in dichloromethane as the oil phase. The water/oil (w/o) emulsion was gradually added to the outer water phase containing polyvinyl alcohol (PVA, 0.1%, w/v), NaCl (2%, w/v) and maltose (2%, w/v) adjusted to pH 3.0, under stirring with a turbine-shaped mixer at 5000 rpm to obtain a water/oil/water emulsion. Then PLGA microspheres were formed in the outer water phase after the evaporation of dichloromethane. In order to recover the microspheres without a free form of ONO-8815Ly, the suspension was centrifuged at 3000 rpm for 10 min and the microspheres were precipitated. The washed microsphere precipital was lyophilized to remove residual organic solvent and water, and then dried solid ONO-8815Ly-loaded microspheres were recovered. ONO-8815Ly-loaded microspheres were dispersed in purified water, and then gelatin aqueous solution (20%, w/w) was poured into the microsphere suspension. The resultant microsphere–gelatin suspension was poured into a polypropylene container and placed in a refrigerator for 12 h to form a gel. Afterward, glutaraldehyde aqueous solution (12.5 μg/ml) was poured into the microsphere–gelatin gel and placed in the refrigerator for 24 h for the crosslink reaction. The gel sheet obtained was placed into glycine aqueous solution. These procedures were performed repeatedly. Small cylinder-shaped gelatin hydrogels containing either 80 or 400 μg of ONO-8815 were obtained by hollowing out the gelatin hydrogel sheet.

SURGICAL PROCEDURE

The institutional animal research committee, according to the guidelines for Animal Experiments of Kyoto University, approved this investigation. Japanese white rabbits (Shimizu Laboratory Supplies Co., Kyoto, Japan) were at least 5 months old and had a body weight of 3 kg.

Two types of cartilage defect on the femoral concave of the patello-femoral joint were made according to depth (Supplementary Fig. 1). A chondral defect, which involved the osteochondral boundary (tide mark) but not subchondral bone, was made using a punch without damaging the subchondral bone (5.0 mm in diameter) [Supplementary Fig. 1(A–C)]. An osteochondral defect was made using a hand drill [4.0 mm in diameter and 5.0 mm in depth, Supplementary Fig. 1(D–F)]. By preliminary experiments, we have confirmed that both types of defects were not healed spontaneously (data not shown).

The same type of defect was created in both femurs, and a cylinder-shaped gelatin hydrogel containing PLGA microspheres conjugated with ONO-8815 (80 or 400 μg) was placed into the infra-patellar fat pad on one side (thereafter designated EP2 agonist-treated samples), and gelatin hydrogels without microspheres were placed on the contralateral side (contralateral samples). The animals were allowed to move. To exclude any possible effect of ONO-8815 in the systemic circulation, controls were established, in which empty gelatin hydrogel was placed in bilateral knee joints after creating each defect model (control samples, $N = 3$). Animals were sacrificed and evaluated at 4 ($N = 5$) and 12 ($N = 8$) weeks after the operation.

HISTOLOGICAL EVALUATION

Cartilage samples were fixed overnight at 4°C in a 10% formalin solution, decalcified by formic acid, and embedded in paraffin. Then sections were cut at 6 mm through the center of each defect, stained with Safranin-O/Fast Green and hematoxylin–eosin (HE), examined in a blinded manner by two evaluators, and graded with the use of a modified Wakitani histological scale[14]. The reconstitution of articular chondrocytes and subchondral bone connections (category II on the modified Wakitani scale) was partially evaluated by grading from 0 to 7. Specimens of the synovium around the infra-patellar fat pads were fixed in 10% formalin, embedded in paraffin, and cut into 6 μm thick sections for histological evaluation. Sections were stained with HE and the severity of synovial lesions was graded according to the histological scoring system, based on the hyperplasia of synovial lining cells, hypertrophy of the synovial lining layer, infiltration of inflammatory cells, proliferation of granulation tissue, and vascularization[15]. Two independent observers blinded to the treatment groups graded all sections.

IMMUNOHISTOCHEMISTRY

Immunostaining of proliferating cell nuclear antigen (PCNA; diluted 1:100; Dako, Glostrup, Denmark) and alpha1 type II collagen (diluted 1:50; Daiichi Fine Chemical, Toyama, Japan) was performed as previously mentioned[11]. Immunostaining of EP2 (diluted 1:100; Cayman Chemical Co., Ann Arbor, MI) was performed as described by Fukuda *et al.*[16]. Under the microscope (400×), all cells and PCNA-positive cells were counted by two individuals. Three visual fields were randomly selected by each observer, and, therefore, each specimen was evaluated three times. Then labeling index was calculated as the mean of these three values. The relative increase in PCNA-positive cells was expressed as the ratio of the labeling index of the EP2 agonist-treated sample vs that of the contralateral sample. The labeling index of control sample was also calculated as a value relative to those of contralateral sample.

ASSAY OF MMP3, TNF-α, AND C-REACTIVE PROTEIN (CRP) IN SYNOVIAL FLUID

After the injection of 1 ml of saline solution into the knee joint, synovial fluid was obtained by arthrocentesis through a sub-patellar approach. Synovial fluid was aspirated as far as possible from the knee joint. After

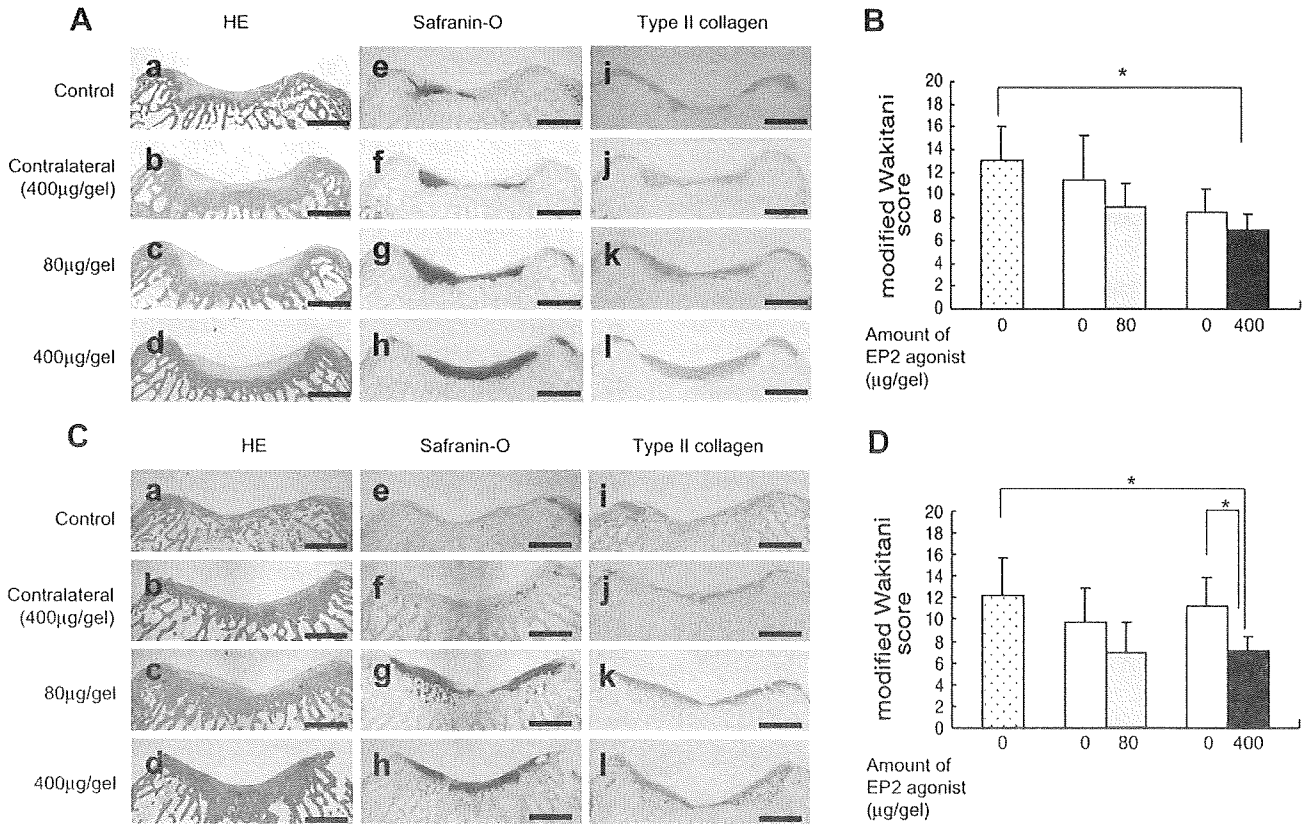

Fig. 1. Effects of EP2 agonist on the regeneration of chondral defects. Histological evaluations were performed at 4 (A) or 12 (C) weeks after the operation. Each specimen was prepared from control samples (a, e, and i), contralateral (b, f, and j), or EP2 agonist-treated (c, g, and k, 80 μg/gel; d, h and l; 400 μg/gel) samples. The quality of regenerated tissues was analyzed by HE staining (a–d), Safranin-O staining (e–h), or immunohistochemical staining with anti-type II collagen Ab (i–l). Magnification 2×. Bar = 2.0 mm. The quality of regenerated tissues was also evaluated with a modified Wakitani histological scale at 4 (B) and 12 (D) weeks after the operation. Dotted and open boxes indicate the scale for control and contralateral samples, respectively, $^*P < 0.05$.

the specimen was centrifuged at 1500 rpm for 20 min, the supernatant was drawn out and stored at −70°C[17]. MMP3 activity was measured with a MMP3 fluorimetric drug discovery kit (BIOMOL International LP, Plymouth Meeting, PA). TNF-α levels in joint fluids were measured using a sandwich enzyme-linked immunosorbent assay (ELISA) with specific anti-TNF-α polyclonal antibodies (Abs) (BD Pharmingen, San Diego, CA). Briefly, microtiter plates were coated with 50 μl of anti-rabbit. TNF-α capture Abs (4 mg/ml) overnight at 4°C, then washed twice with phosphate buffered saline (PBS) containing 0.05% Tween 20 and blocked overnight at 4°C with 10% fetal bovine serum (FBS) in PBS. After the plates were washed four times, standards and samples (100 μl) were incubated in duplicate overnight at 4°C. Plates were again washed and a biotin-conjugated anti-TNF-α secondary Ab (2 mg/ml) was added for 1 h at room temperature. A 30-min incubation with a 1:400 dilution of avidin–peroxidase (Sigma) followed extensive washing of the plate. Finally, TMBlue (Intergen, Milford, MA) substrate was added (100 μl/well) and incubated at room temperature for 30 min. The absorbance was read at 450 nm with an UVmax microplate reader (Molecular Devices, Menlo Park, CA). Rabbit CRP was measured with a rabbit CRP ELISA kit (Alpha Diagnostic International Inc., San Antonio, TX).

REVERSE TRANSCRIPTION-POLYMERASE CHAIN REACTION (RT-PCR)

Total RNA was extracted from frozen synovial samples using TRIzol reagent (Invitrogen, Carlsbad, CA) and 1 μg was reverse transcribed for single-stranded cDNA using the oligo (dT) primer and Superscript II reverse transcriptase (Invitrogen). RT-PCR was performed in duplicate for each sample using primers listed in Table I[18,19].

Table I
Primers used in the RT-PCR analyses

Gene	Primers*	Size (bp)	Position	Accession no.
MMP3	CTGGAGGTTTGATGAGAAGA CAGTTCATGCTCGAGATTCC	336	1278–1297 1597–1616	NM_001082280
TIMP1	GCAACTCCGACCTTGTCATC AGCGTAGGTCTTGGTGAAGC	326	122–141 428–447	NM_001082232
IL-1β	TGCTGTCCAGACGAGGGCAT ACTCTCCAGCTGCAGGGTAG	473	210–229 664–683	NM_001082201
GAPDH	GTCAAGGCTGAGAACGGGAA GCTTCACCACCTTCTTGATG	613	246–265 839–858	NM_001082253

*All primer sequences are written from 5′ to 3′. The top sequence is the sense primer and the bottom sequence is the anti-sense primer.

QUANTITATIVE RT-PCR

The levels of mRNA expression of genes (*MMP3*, *TIMP1*, *IL-1β* and *glyceraldehyde 3-phosphate dehydrogenase* (*GAPDH*)) were quantified by SYBR Green (Applied Biosystems, Foster City, CA) real time PCR with the ABI PRISM 377 Sequence Detection System (Applied Biosystems). Each gene amplification efficiency was similar with *GAPDH*. All reactions were run in triplicate, and the mean value was used to calculate the ratio of target gene/*GAPDH* expression in each sample. Using the ratio in untreated sample as a standard (1.0), the relative ratio of the treated sample was presented as the relative expression level of the target gene[11].

STATISTICAL ANALYSES

All statistical analyses were performed using Statcel software. The results are shown as the mean ± SD. The analysis of variance (ANOVA) test was used to compare the differences in the scales between multiple groups. The Student's *T* test was used to compare the differences in the scales between two groups. A P value < 0.05 was considered significant.

Results

EP2 AGONIST PROMOTED TISSUE REGENERATION IN THE CHONDRAL DEFECT MODEL

Four weeks after the operation, the quality of regenerated tissues was analyzed by HE staining [Fig. 1(A, a–d)], Safranin-O staining [Fig. 1(A, e–h)], or immunohistochemical staining with anti-type II collagen Ab [Fig. 1(A, i–l)]. Most of regenerated tissues in EP2 agonist-treated samples were Safranin-O-positive and type II collagen-positive, suggesting the quality as hyaline cartilage. The quality of regenerated tissue evaluated by modified Wakitani histological scale was much better in EP2 agonist-treated samples than control samples, and the difference was statistically significant in the case of 400 μg/gel-treated samples [Fig. 1(B): 80 μg, $P = 0.08$; 400 μg, $P = 0.04$]. On the other hand, there were no statistically significant difference in histological scale between EP2 agonist-treated and contralateral samples [Fig. 1(B): 80 μg, $P = 0.21$; 400 μg, $P = 0.24$].

The effect of EP2 agonist treatment was much clear at 12 weeks after operation. In control and contralateral samples, the amount of regenerated tissues was much less than that found at 4 weeks after operation, and most of them were negative for Safranin-O or type II collagen [Fig. 1(C)]. In EP2 agonist-treated samples, regenerated tissues reached a considerable width, most of which were Safranin-O and type II collagen-positive indicating properties compatible with hyaline cartilage [Fig. 1(C)]. The histological scale of EP2 agonist-treated samples showed significantly better than that of control and also contralateral samples in the case of 400 μg/gel-treated

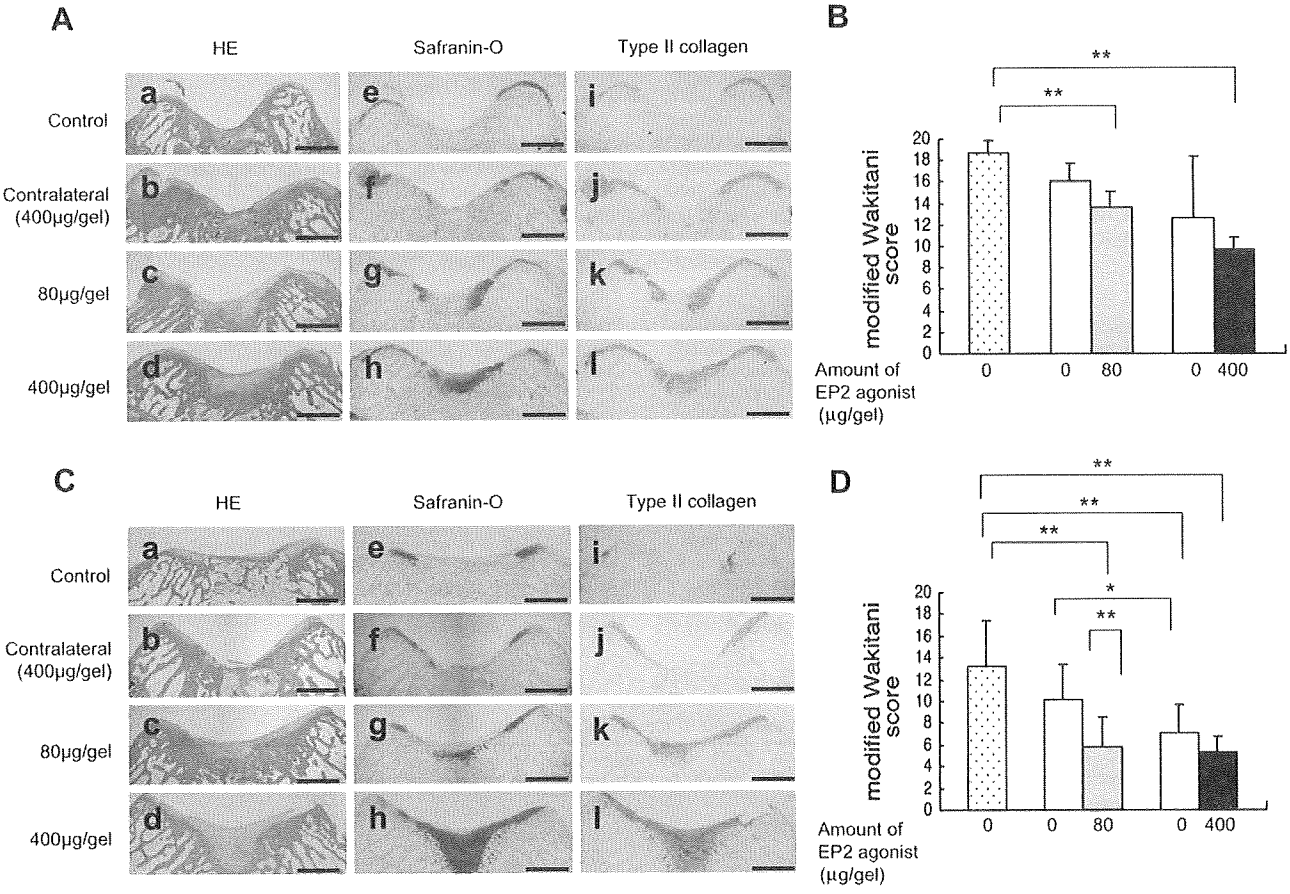

Fig. 2. Effects of EP2 agonist on the regeneration of osteochondral defects. Histological evaluations were performed at 4 (A) or 12 (C) weeks after the operation. Each specimen was prepared from control samples (a, e, and i), contralateral (b, f, and j), or EP2 agonist-treated (c, g, and k, 80 μg/gel; d, h and l; 400 μg/gel) samples. The quality of regenerated tissues was analyzed by HE staining (a–d), Safranin-O staining (e–h), or immunohistochemical staining with anti-type II collagen Ab (i–l). Magnification 2×. Bar = 2.0 mm. The quality of regenerated tissues was also evaluated with a modified Wakitani histological scale at 4 (B) and 12 (D) weeks after the operation. Dotted and open boxes indicate the scale for control and contralateral samples, respectively, $^{**}P < 0.01$; $^{*}P < 0.05$.

samples [Fig. 1(D): vs control, $P = 0.02$; vs contralateral, $P = 0.01$]. The histological scale of contralateral samples tended to be better than that of control samples, although there was no statistical significance [Fig. 1(C): 80 μg, $P = 0.31$; 400 μg; $P = 0.1$, Fig. 1(D): 80 μg, $P = 0.2$; 400 μg; $P = 0.35$].

EP2 AGONIST PROMOTED TISSUE REGENERATION IN THE OSTEOCHONDRAL DEFECT MODEL

To analyze the effect of the EP2 agonist on tissue regeneration in osteochondral lesions, an osteochondral defect model was created [Supplementary Fig. 1(C–E)]. At 4 weeks

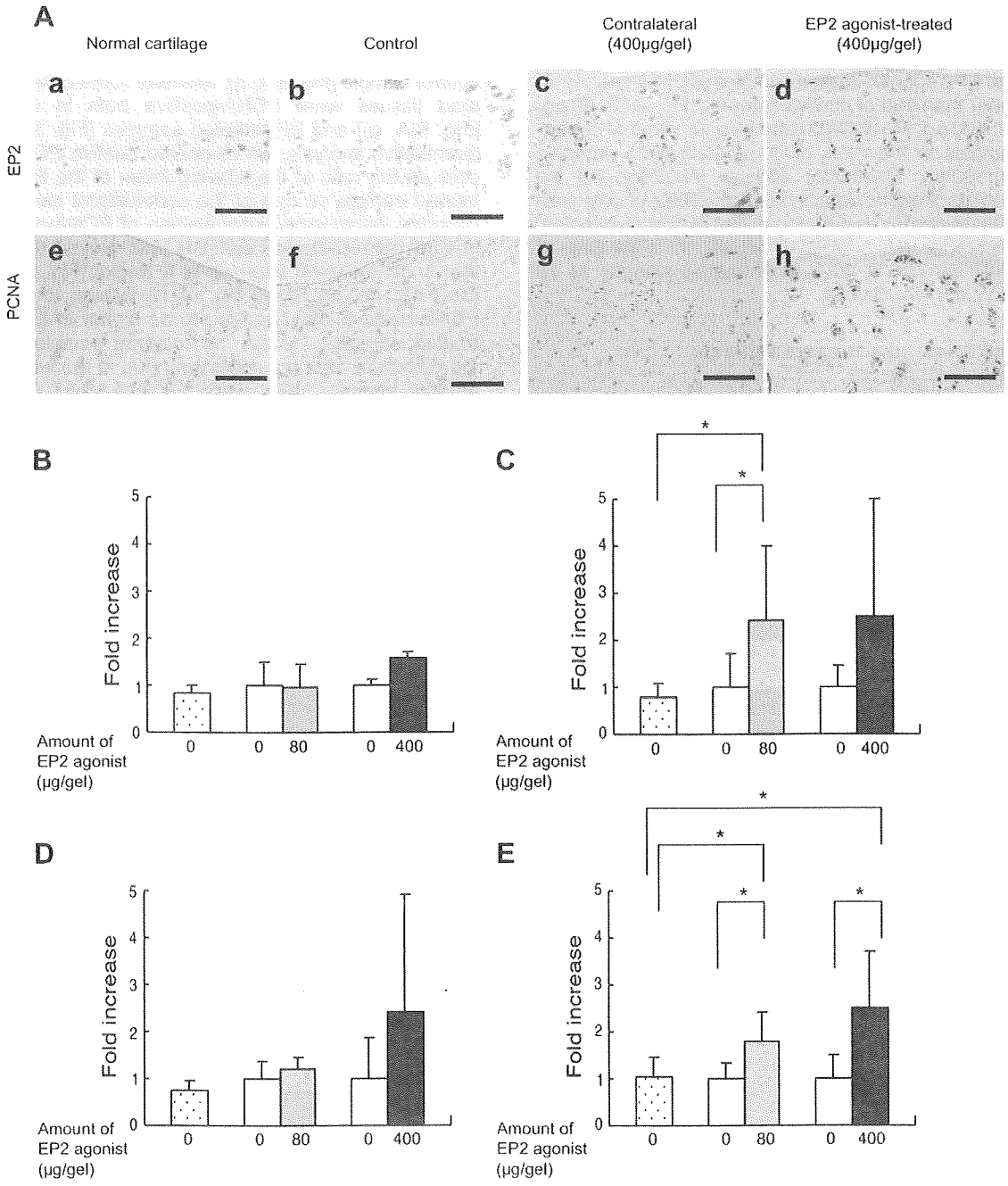

Fig. 3. EP2 agonist promotes proliferation of EP2-positive cells. A: Expression of EP2 and PCNA in normal and regenerated cartilage of chondral defect model. Specimens were prepared from a normal femur without any treatment (a and e), a control sample (b and f), a contralateral sample (c and g), and an EP2 agonist-treated (400 μg/gel) sample (d and h) at 12 weeks after the operation. Immunohistochemical staining was performed with anti-EP2 Ab (a–d) or anti-PCNA Ab (e–h). Bar = 100 μm. B–E: Quantitative analysis of PCNA-positive cells. Cells positive for PCNA staining were counted under the microscope, and a labeling index was calculated for each sample. The relative increase in PCNA-positive cells is expressed as the ratio of the labeling index of the EP2 agonist-treated sample (shaded bars) vs that of the contralateral sample (open bars). The labeling index of control sample relative to those of contralateral sample was indicated in dotted boxes. Samples were prepared from the chondral defect model at 4 weeks (B), chondral defect model at 12 weeks (C), osteochondral defect model at 4 weeks (D), and osteochondral defect model for 12 weeks (E), $^*P < 0.05$.

after the operation, the osteochondral defects were filled with regenerated tissue in all cases, but there was a significant difference in histological scale between EP2 agonist-treated and control samples [Fig. 2(D): 80 μg, $P = 0.005$; 400 μg, $P = 0.0003$]. As in the chondral defect model, the difference was not significant between EP2 agonist-treated than contralateral samples [Fig. 2(D): 80 μg, $P = 0.07$; 400 μg, $P = 0.21$].

At 12 weeks after operation, the effect of EP2 agonist treatment was much evident. The osteochondral defect of EP2 agonist-treated samples was filled with Safranin-O and type II collagen-positive tissues [Fig. 2(C)], and the grading scale of EP2 agonist-treated samples showed and significantly better than that of control samples [Fig. 2(D): 80 μg, $P = 0.002$; 400 μg, $P = 0.0003$] and also than that of contralateral samples in the case of 80 μg/gel-treated samples [Fig. 2(D): 80 μg, $P = 0.006$; 400 μg, $P = 0.05$]. As we observed in the chondral defect model, the scale of contralateral samples tended to be better than that of control samples, and the difference was statistically significant in the case of contralateral sample in 400 μg/gel-treated animals at 12 weeks [Fig. 2(D), $P = 0.005$].

EP2 AGONIST STIMULATED THE PROLIFERATION OF EP2-POSITIVE CELLS

In normal cartilage, almost all cells were EP2-positive as we previously demonstrated in mice and human articular cartilage[11] [Fig. 3(A, a)]. Almost all cells in regenerated tissues of chondral defect model at 12 weeks after operation expressed the EP2 receptor in control [Fig. 3(A, b)], contralateral [Fig. 3(A, c)] and EP2-treated samples (400 μg/gel) [Fig. 3(A, d)]. Identical results were observed in samples harvested at 12 weeks after operation (data not shown), suggesting that the cartilage regeneration was conducted mainly by EP2-positive cells. To evaluate the proliferating ability of these EP2-positive cells, same specimens were used for PCNA staining [Fig. 3(A, e–h)]. Almost no cells were PCNA-positive in normal cartilage [Fig. 3(A, e)] and control sample [Fig. 3(A, f)], whereas some cells in regenerated tissues were PCNA-positive both in contralateral [Fig. 3(A, g)] and EP2-treated samples [Fig. 3(A, h)]. For quantitative analysis, we compared relative PCNA-positive cells as the ratio of the labeling index of the EP2 agonist-treated sample vs that of the contralateral sample. In the chondral defect model, the fraction of PCNA-positive cells in EP2 agonist-treated samples was almost the same as that in contralateral samples at 4 weeks [Fig. 3(B): 80 μg, $P = 0.47$; 400 μg, $P = 0.19$]. At 12 weeks, the fraction of PCNA-positive cells seemed to be higher in EP2 agonist-treated samples than in contralateral samples, although the difference was not convincing due to the wide variation among samples [Fig. 3(C): 80 μg, $P = 0.04$; 400 μg, $P = 0.12$]. In the osteochondral defect model, the fraction of PCNA-positive cells in EP2-treated samples was not

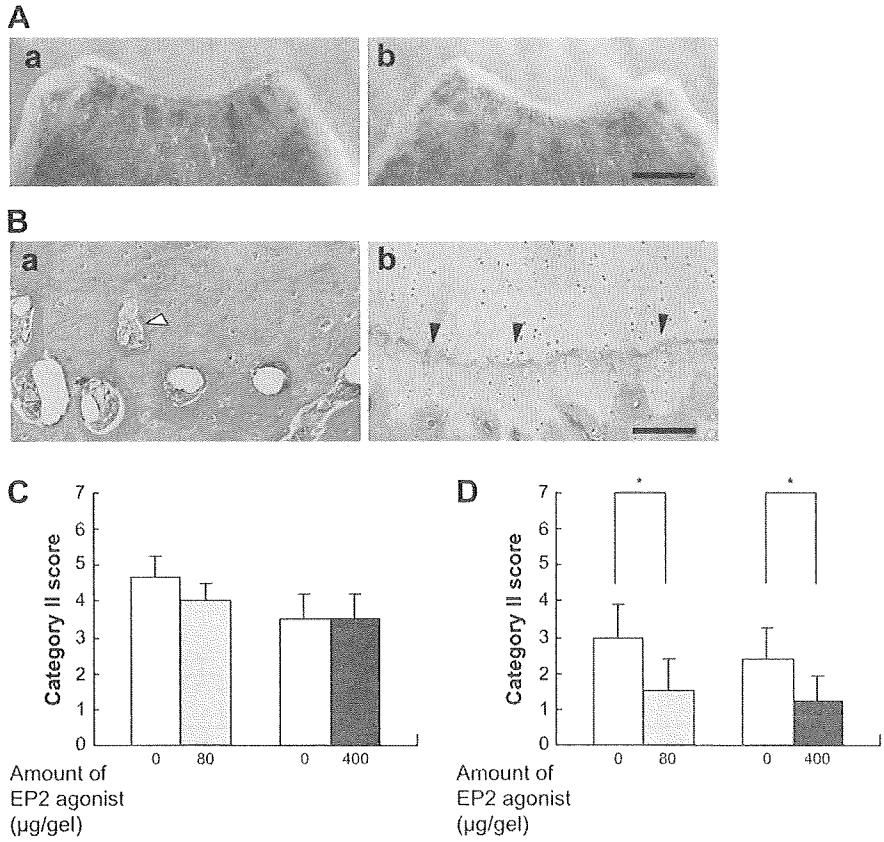

Fig. 4. Effect of EP2 agonist on remodeling of the deep layer zone in chondral defect model. A: Macroscopic view of specimens from contralateral sample (a) and EP2 agonist-treated (400 μg/gel) sample (b) of chondral defect model at 12 weeks after the operation. Bar = 4.0 mm. B: Microscopic view of the osteochondral boundary in the specimens presented in (A). (a) Contralateral sample, (b) EP2 agonist-treated (400 μg/gel) sample. Note that there was no clear boundary, and vascular invasion into articular chondrocytes (white arrowhead) was observed in (a), whereas a clear tidemark (black arrowhead) was formed in (b). Magnification 40×. Bar = 100 μm. C and D: Quantitative evaluation of the osteochondral boundary. The boundary formed between articular cartilage and subchondral bone was evaluated by category II scale of the modified Wakitani scale (0–7, 7 is worse). Samples were prepared from the chondral defect model at 4 weeks (C) and at 12 weeks (D), $^*P < 0.05$.

different from those in contralateral samples at 4 weeks [Fig. 3(D): 80 μg, $P = 0.31$; 400 μg, $P = 0.46$], but significantly higher at 12 weeks [Fig. 3(E): 80 μg, $P = 0.02$; 400 μg, $P = 0.02$]. In all settings, the labeling index of control samples showed no difference from those of contralateral samples [Fig. 3(B): $P = 0.47$; Fig. 3(C): $P = 0.31$; Fig. 3(D): $P = 0.1$; Fig. 3(E): $P = 0.43$].

EP2 AGONIST REPAIRED THE OSTEOCHONDRAL BOUNDARY

Reconstruction of the physiological boundary between articular cartilage and underlying bone tissue is important to maintain the mechanical and biological properties of articular cartilage. Macroscopical examination of EP2 agonist-treated (400 μg/gel) samples in chondral defect model at 12 weeks after operation showed a clear boundary between articular cartilage and subchondral bone [Fig. 4(A, b)]. Microscopical examination demonstrated the reconstruction of the tidemark [Fig. 4(B, b)]. These findings were not observed in contralateral samples. The boundary was not clear in macroscopical examination [Fig. 4(A, a)], and microscopical examination also showed no boundary with some vascular structures in the cartilaginous portion [Fig. 4(B, a)]. The difference was quantitatively evaluated using the category II scale of the modified Wakitani scale. There was no significant difference between EP2 agonist-treated and contralateral samples at 4 weeks [Fig. 4(C)], but the scale was significantly lower in the former than the latter at 12 weeks after operation [Fig. 4(D): 80 μg, $P = 0.03$; 400 μg, $P = 0.04$].

Similar findings were obtained in the osteochondral defect model (Fig. 5). EP2 agonist-treated (400 μg/gel) samples in osteochondral defect model at 12 weeks after operation the showed a clear boundary between articular cartilage and subchondral bone by macroscopical and microscopical examinations [Fig. 5(A, b and B, b)], which were not observed in contralateral samples [Fig. 5(A, a and B, a)]. Quantitative evaluation demonstrated that the boundary was much better formed in 400 μg/gel-, but not 80 μg/gel-treated samples than in contralateral samples at 12 weeks after operation [Fig. 5(D): 80 μg, $P = 0.07$; 400 μg, $P = 0.009$]. This difference was not observed in samples at 4 weeks [Fig. 5(C)]. These results suggest that the EP2 agonist improved the environment surrounding cartilage.

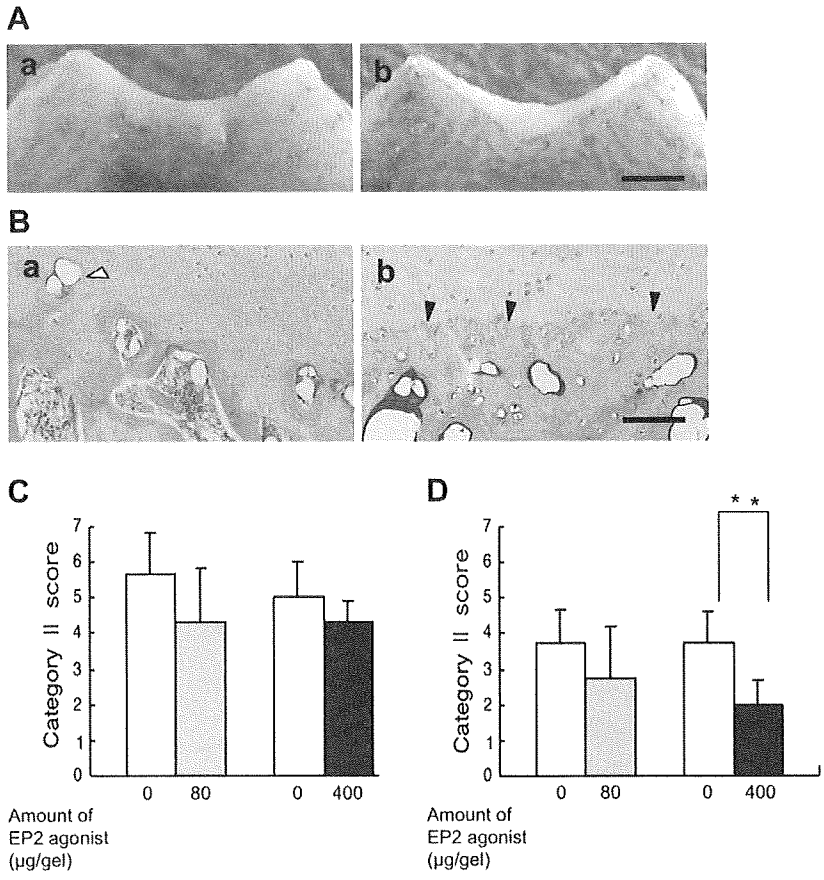

Fig. 5. Effect of EP2 agonist on remodeling of the deep layer zone in osteochondral defect model. A: Macroscopic view of specimens from contralateral sample (a) and EP2 agonist-treated (400 μg/gel) sample (b) of osteochondral defect model at 12 weeks after the operation. Bar = 4.0 mm. B: Microscopic view of the osteochondral boundary in the specimens presented in (A). (a) Contralateral sample (b) EP2 agonist (400 μg/gel)-treated sample. Note that there was no clear boundary, and vascular invasion into articular chondrocytes (white arrowhead) was observed in (a), whereas a clear tidemark (black arrowhead) was formed in (b). Magnification 40×. Bar = 100 μm. C and D: Quantitative evaluation of the osteochondral boundary. The boundary formed between articular cartilage and subchondral bone was evaluated by category II scale of the modified Wakitani scale (0–7, 7 is worse). Samples were prepared from the chondral defect model at 4 weeks (C) and at 12 weeks (D), $^{**}P < 0.01$.